



Essential Welding Variables

Final Report 278-T-06

For Project

Development of Optimized Welding Solutions for X100 Line Pipe Steel

Prepared for the

Design, Materials, and Construction Technical Committee of
Pipeline Research Council International, Inc.
Project MATH-1 Catalog No. L5XXXX

And

U.S. Department of Transportation
Pipeline and Hazardous Materials Safety Administration
Office of Pipeline Safety
Agreement Number DTPH56-07-T-000005

Prepared by
V.B. Rajan
The Lincoln Electric Company

September 2011

This research was funded in part under the Department of Transportation, Pipeline and Hazardous Materials Safety Administration's Pipeline Safety Research and Development Program. The views and conclusions contained in this document are those of the authors and should not be interpreted as representing the official policies, either expressed or implied, of the Pipeline and Hazardous Materials Safety Administration, or the U.S. Government.



Catalog No. L5XXXX

Essential Welding Variables

Final Report 278-T-06

For Project

Development of Optimized Welding Solutions for X100 Line Pipe Steel

Prepared for the

Design, Materials, and Construction Technical Committee of
Pipeline Research Council International, Inc.
Project MATH-1 Catalog No. L5XXXX

And

U.S. Department of Transportation
Pipeline and Hazardous Materials Safety Administration
Office of Pipeline Safety
Agreement Number DTPH56-07-T-000005

Prepared by

V.B. Rajan

The Lincoln Electric Company

September 2011

Version	Date of Last Revision	Date of Uploading	Comments
2	March 2011	4 April 2011	References to be inserted after review.
Final	September 2011	September 2011	

This report is furnished to Pipeline Research Council International, Inc. (PRCI) under the terms of PRCI contract [278-PR- 348 - 074513], between PRCI and the MATH-1 contractors:

- Electricore (prime contractor),
- Center for Reliable Energy Systems, CANMET, NIST, and The Lincoln Electric Company (sub-contractors).

The contents of this report are published as received from the MATH-1 contractor and subcontractors. The opinions, findings, and conclusions expressed in the report are those of the authors and not necessarily those of PRCI, its member companies, or their representatives. Publication and dissemination of this report by PRCI should not be considered an endorsement by PRCI of the MATH-1 contractor and subcontractors, or the accuracy or validity of any opinions, findings, or conclusions expressed herein.

In publishing this report, PRCI and the MATH-1 contractors make no warranty or representation, expressed or implied, with respect to the accuracy, completeness, usefulness, or fitness for purpose of the information contained herein, or that the use of any information, method, process, or apparatus disclosed in this report may not infringe on privately owned rights. PRCI and the MATH-1 contractors assume no liability with respect to the use of, or for damages resulting from the use of, any information, method, process, or apparatus disclosed in this report. By accepting the report and utilizing it, you agree to waive any and all claims you may have, resulting from your voluntary use of the report, against PRCI and the MATH-1 contractors.

Pipeline Research Council International Catalog No. L5XXXX

PRCI Reports are Published by Technical Toolboxes, Inc.

3801 Kirby Drive, Suite 520
Houston, Texas 77098
Tel: 713-630-0505
Fax: 713-630-0560
Email: info@ttoolboxes.com

PROJECT PARTICIPANTS

PROJECT TEAM MEMBER	COMPANY AFFILIATION	PROJECT TEAM MEMBER	COMPANY AFFILIATION
Arti Bhatia	Alliance	Jim Costain	GE
Jennifer Klementis	Alliance	Gilmar Batista	Petrobras
Roger Haycraft	Boardwalk	Marcy Saturno de Menezes	Petrobras
David Horsley	BP	Dave Aguiar	PG&E
Mark Hudson	BP	Ken Lorang	PRCI
Ron Shockley	Chevron	Maslat Al-Waranbi	Saudi Aramco
Sam Mishael	Chevron	Paul Lee	SoCalGas
David Wilson	ConocoPhillips	Alan Lambeth	Spectra
Satish Kulkarni	El Paso	Robert Turner	Stupp
Art Meyer	Enbridge	Gilles Richard	TAMSA
Bill Forbes	Enbridge	Noe Mota Solis	TAMSA
Scott Ironside	Enbridge	Philippe Darcis	TAMSA
Sean Keane	Enbridge	Dave Taylor	TransCanada
Laurie Collins	Evraz	Joe Zhou	TransCanada
David de Miranda	Gassco	Jason Skow	TransGas
Adriaan den Herder	Gasunie	Ernesto Cisneros	Tuberia Laguna
Jeff Stetson	GE	Vivek Kashyap	Welpsun
		Chris Brown	Williams

CORE RESEARCH TEAM	
RESEARCHER	COMPANY AFFILIATION
Yaoshan Chen	Center for Reliable Energy Systems
Yong-Yi Wang	Center for Reliable Energy Systems
Ming Liu	Center for Reliable Energy Systems
Dave Fink	Lincoln Electric Company
Marie Quintana	Lincoln Electric Company
Vaidyanath Rajan	Lincoln Electric Company
Joe Daniel	Lincoln Electric Company
Radhika Panday	Lincoln Electric Company
James Gianetto	CANMET Materials Technology Laboratory
John Bowker	CANMET Materials Technology Laboratory
Bill Tyson	CANMET Materials Technology Laboratory
Guowu Shen	CANMET Materials Technology Laboratory
Dong Park	CANMET Materials Technology Laboratory
Timothy Weeks	National Institute of Standards and Technology
Mark Richards	National Institute of Standards and Technology
Dave McColskey	National Institute of Standards and Technology
Enrico Lucon	National Institute of Standards and Technology
John Hammond	Consultant Metallurgist & Welding Engineer

This Page Intentionally Left Blank

FINAL REPORT STRUCTURE

Focus Area 1 - Update of Weld Design, Testing, and Assessment Procedures for High Strength Pipelines		
Report #	Description	Lead Authors
277-T-01	Background of Linepipe Specifications	CRES/CANMET
277-T-02	Background of All-Weld Metal Tensile Test Protocol	CANMET/Lincoln
277-T-03	Development of Procedure for Low-Constraint Toughness Testing Using a Single-Specimen Technique	CANMET/CRES
277-T-04	Summary of Publications: Single-Edge Notched Tension SE(T) Tests	CANMET
277-T-05	Small Scale Tensile, Charpy V-Notch, and Fracture Toughness Tests	CANMET/NIST
277-T-06	Small Scale Low Constraint Fracture Toughness Test Results	CANMET/NIST
277-T-07	Small Scale Low Constraint Fracture Toughness Test Discussion and Analysis	CANMET/NIST
277-T-08	Summary of Mechanical Properties	CANMET
277-T-09	Curved Wide Plate Tests	NIST/CRES
277-T-10	Weld Strength Mismatch Requirements	CRES/CANMET
277-T-11	Curved Wide Plate Test Results and Transferability of Test Specimens	CRES/CANMET
277-S-01	Summary Report 277 Weld Design, Testing, and Assessment Procedures for High Strength Pipelines	CRES

Focus Area 2 - Development of Optimized Welding Solutions for X100 Linepipe Steel		
Report #	Description	Lead Authors
278-T-01	State of The Art Review	Lincoln
278-T-02	Material Selection, Welding and Weld Monitoring	Lincoln/CANMET
278-T-03	Microstructure and Hardness Characterization of Girth Welds	CANMET/Lincoln
278-T-04	Microstructure and Properties of Simulated Weld Metals	CANMET/Lincoln
278-T-05	Microstructure and Properties of Simulated Heat Affected Zones	CANMET/Lincoln
278-T-06	Essential Welding Variables	Lincoln/CANMET
278-T-07	Thermal Model for Welding Simulations	CRES/CANMET
278-T-08	Microstructure Model for Welding Simulations	CRES/CANMET
278-T-09	Application to Other Processes	Lincoln/CANMET
278-S-01	Summary Report 278 Development of Optimized Welding Solutions for X100 Line Pipe Steel	Lincoln

EXECUTIVE SUMMARY

This is the sixth in the series of nine topical reports that detail the research leading to the development of the optimized welding solutions for X100 line pipe steel. Collectively, these reports have highlighted the essential welding variables and the methodology for monitoring and controlling them.

In this report, the essential welding variables are examined in greater detail. Initial identification of the primary variables was accomplished using a thermal-microstructural model. The outputs from this model were used in developing a statistical test matrix for welding experiments in flattened X100 pipe to validate and corroborate the identification of the primary welding variables. Significant linear models were obtained between the welding variables such as weld composition, preheat/interpass temperature, True Heat Input, torch configuration and weld mechanical properties such as yield strength, tensile strength, hardness and Charpy toughness and the 800^oC to 500^oC cooling times (t_{85}) in the heat affected zone (HAZ). Results indicated that the weld composition was the most influential in increasing the weld strength and hardness, followed by torch configuration, preheat/interpass temperature and True Heat Input, whereby going from dual to single torch, decreasing preheat/interpass temperatures and decreasing true heat input increased weld metal strength and hardness. Groove bevel offset was not identified as a significant factor. Charpy toughness increased with increasing preheat/interpass temperatures and leaner weld composition. The heat affected zone t_{85} cooling times increased significantly in going from single to dual torch configuration, and increasing preheat/interpass temperatures and true heat input.

Development of the statistically significant models enabled the development of transfer functions correlating the welding variables to mechanical properties, which enabled the development of control methodology for the essential welding variables. This methodology utilized the transfer functions to limit the maximum variation in hardness, yield and tensile strengths to $\pm 2\%$ due to variation in the welding input variables. This enabled definition of the envelope of welding input variables such as preheat and interpass temperatures, True Heat Input, wire feed speed/travel speed ratio and contact tip to work distance (CTWD). This control methodology was applied to actual 5G welding in fabrication shops to simulate field welding of X100 pipe.

Shop welding experience indicated that this control methodology could be implemented in X100 welding, provided True Heat Input is carefully monitored and controlled around the pipe, and the other variables are controlled within well defined limits. Two different contractors A and B and two different X-100 pipe grades A and B were utilized in 5G welding experiments in the fabrication shops. Apart from occasional variation in True Heat Input as a function of clock position with contractor A, the control methodology was followed quite effectively by both contractors. In general, the properties obtained with both contractors were quite consistent. Minor variation of properties was seen with clock position which was a result of the differences in penetration patterns in the welds as a function of clock position. In summary, successful application of the control methodology for the essential welding variables was found to reduce variation in weld mechanical properties around the pipe

TABLE OF CONTENTS

EXECUTIVE SUMMARY	vii
TABLE OF CONTENTS.....	viii
LIST OF FIGURES	ix
LIST OF TABLES.....	x
ABSTRACT.....	xi
1 INTRODUCTION	1
1.1 Background	1
1.2 Integrated Thermal-Microstructure Model.....	2
2 TECHNICAL APPROACH.....	2
2.1 Design of Experiment (DOE) - Virtual Simulations.....	3
2.2 Design of Experiment - Plate Welding (DOE).....	4
2.3 Methodology for the Recommendation of Essential Variables	7
3 RESULTS AND DISCUSSION	7
3.1 Virtual Experiments	7
3.1.1 Weld Metal Hardness Predictions.....	7
3.1.2 HAZ Cooling Time Predictions	10
3.2 Plate Experiment Results	11
3.3 Control of Essential Variables.....	20
3.4 Application of Essential Variable Control to Field Welding Conditions.....	21
3.5 Tensile & Hardness Results	25
3.6 Impact Toughness	33
4 CONCLUSIONS.....	35
5 REFERENCES	38
6 APPENDIX 1.....	40
7 APPENDIX 2.....	42

LIST OF FIGURES

Figure 1. Correlation between the microhardness across the tensile specimen cross section and its average value compared to the 0.2% offset yield (YS), flow stress (FS) and tensile strength (TS) observed in 807F 1G weld from the first round of welding	4
Figure 2. Average Hardness vs. 800 ⁰ C to 500 ⁰ C cooling time from the weld metal Gleeble simulation experiments.	5
Figure 3. Schematic representations of Traditional GMAW-P and RapidArc® waveforms	6
Figure 4: Hardness Distributions from Virtual Simulations	8
Figure 5: Effect of joint offset and torch configuration on average centerline weld hardness True Heat Input= 0.53 kJ/mm (13.5 kJ/in.), Pcm=0.29, PHT/INT=104	8
Figure 6: Effect of preheat / interpass and consumable composition, Pcm, on average centerline weld hardness True Heat Input= 0.53 kJ/mm (13.5 kJ/in.), Offset=0.10, Single Torch	9
Figure 7. HAZ t85 cooling predictions with true and average heat input compared to experimental results	10
Figure 8: : Effect of preheat / interpass temperatures and True Heat Input on HAZ t85 cooling times	10
Figure 9: Effect of preheat / interpass temperatures and groove offset on HAZ t85 cooling times	11
Figure 10. Effect of Preheat/Interpass Temperature and Weld Composition on Average Weld Centerline Hardness	13
Figure 11. Effect of True Heat Input and Weld Composition on Average Weld Centerline Hardness	13
Figure 12. Effect of Torch configuration and Weld Composition on Average Weld Centerline Hardness	14
Figure 13. Effect of Preheat/Interpass and Composition on Weld Tensile Strength	15
Figure 14. Effect of True Heat Input and Composition on Weld Tensile Strength	15
Figure 15. Effect of Torch configuration and Weld Composition on Weld Tensile Strength	16
Figure 16. Effect of Preheat/Interpass Temperature and Weld Composition on Weld Yield Strength	16
Figure 17. Effect of True Heat Input and Composition on Weld Yield Strength	17
Figure 18. Effect of Torch configuration and Weld Composition on Weld Yield Strength	17
Figure 19. Effect of Preheat/Interpass Temperature and True Heat Input on t85 cooling times in the HAZ near fill pass 2.	18
Figure 20. Effect of Torch configuration and preheat and interpass temperature on t85 cooling times in the HAZ near fill pass 2.....	19
Figure 21. Effect of Preheat/Interpass Temperature and True Heat Input on Charpy Impact Toughness at -20°C....	19
Figure 22. Effect of Torch configuration and Weld Composition on Charpy Impact Toughness at -20°C.....	20
Figure 23. Optimization graph relating yield and tensile strength to preheat/interpass temperatures and True Heat Input values for a single torch weld with a composition indicated by Pcm=0.22.....	21
Figure 24. Variation of True Heat Input with clock position, Weld 952-D fill pass 2	23
Figure 25. Variation of True Heat Input with clock position, Weld #4 Fill Pass 1.....	25
Figure 26. 952-D Stress-Strain Curves and Microhardness Maps (single torch, PT1)	26
Figure 27. 952-F Stress-Strain Curves and Microhardness Maps (single torch, PT1).....	27
Figure 28. Weld 3 Stress-Strain Curves and Microhardness Maps (single torch, PT1).....	28
Figure 29. Weld 4 Stress-Strain Curves and Microhardness Maps (single torch, PT1).....	29
Figure 30. 0.2% Offset Yield Strength, 1% Flow Stress and Tensile Strengths vs. True Heat Input – Contractor A	31
Figure 31. 0.2% Offset Yield Strength, 1% Flow Stress and Tensile Strengths vs. True Heat Input – Contractor B.	31
Figure 32. Transverse Microhardness of Single Torch Welds 952-D & 952-F @ 12 o'clock - Contractor A	32
Figure 33. Transverse Microhardness Traverse of Single Torch Welds 3 & Weld 4 @ 12 0'clock - Contractor B.....	32
Figure 34. Charpy v-notch impact strength as a function of True Heat Input and Clock Position – Contractor A	34
Figure 35. Charpy v-notch impact strength as a function of True Heat Input and Clock Position – Contractor B.....	34

LIST OF TABLES

Table 1. Transfer Functions from DOE Plate Welds	12
Table 2. Pipe Welding Procedures Under Field Welding Conditions	22
Table 3. True Heat Input values (kJ/mm) in weld 952-D	23
Table 4. True Heat Input values (kJ/mm) in weld 952-F	24
Table 5. True Heat Input values (kJ/in) in weld 3	24
Table 6. True Heat Input values (kJ/in) in weld 4	24
Table 7. Chemical Composition of Single Torch Welds made during Shop Welding to mimic Field Welding.....	36
Table 8. Mechanical Properties of Single Torch Welds made during Shop Welding to mimic Field Welding.....	37



TECHNICAL REPORT

No. TH-230

FROM

**The Lincoln Electric
Company**

05 April 2011

V.B. Rajan

PREPARED FOR

**Pipeline Research
Council International
(PRCI)**

**&
Pipeline Hazardous
Materials Safety
Administration
(PHMSA)**

PRCI MATH-1 PHMSA DTPH56-07-T-000005 Development of Optimized Welding Solutions for X100 Line Pipe Steel Topical Report 278-T-06 Essential Welding Variables

ABSTRACT

This is the sixth in the series of nine topical reports that detail the research leading to the development of the optimized welding solutions for X100 line pipe steel. Collectively, these reports have highlighted the essential welding variables and the methodology for monitoring and controlling them.

In this report, the essential welding variables are examined in greater detail. Initial identification of the primary variables was accomplished using a thermal-microstructural model. The outputs from this model were used in developing a statistical test matrix for welding experiments in flattened X100 pipe to validate and corroborate the identification of the primary welding variables. Results indicated that the weld composition, preheat/interpass temperature, True Heat Input and torch configuration were primary variables, whereas the groove bevel offset was not a significant factor. Transfer functions correlating these variables to mechanical properties enabled the development of control methodology for the essential welding variables. This control methodology was applied to actual 5G welding in fabrication shops to simulate field welding of X100 pipe.

Field welding experience indicated that this control methodology could be implemented in X100 welding, provided True Heat Input is carefully monitored and controlled around the pipe, and the other variables are controlled within well defined limits. Successful application of the control methodology for the essential welding variables was found to reduce variation in weld mechanical properties around the pipe.

KEYWORDS

GMAW-P, X100 pipe welding, weld metal, HAZ, essential welding variables, True Power, True Heat Input, Average Heat Input, True Energy™

1 INTRODUCTION

Earlier work on X100 pipe welding concluded that the weld metal properties with the desired level of strength and toughness could be achieved with pulsed gas metal arc welding (GMAW-P) in narrow precision machined grooves [1-6]. However, these properties have been found to be very dependent on the variation in welding parameters and the interaction of these parameters with consumable chemical compositions [3, 4]. Welding parameters such as preheat and interpass temperature, bevel design, torch type (single vs. dual), torch spacing, heat input, power source type and model, consumable and pipe composition have all been mentioned as essential variables that need to be closely controlled to obtain the desired weld properties [1-4, 6]. For example, it had been reported that changing the bevel geometry even with the same welding consumable could produce significantly different weld properties [7]. In addition, the location of the test sample in the weld was found to contribute to variation in the measured mechanical properties [7, 8]. These observations highlight the complexity in understanding the effect of the welding variables on the properties of X100 girth welds. An approach to simplify the identification of essential welding variables is needed to increase the feasibility of reliable X100 pipeline deployment for stress based and especially strain based applications. This report covers the selection and establishment of the essential welding variables and their effect on the weld mechanical properties.

1.1 Background

The work in this project [9, 10] and earlier studies had established that, in addition to consumable (or weld) composition and pipe compositions, the cooling rate from 800⁰C to 500⁰C or even 800⁰C to 400⁰C has a profound effect on the evolution of microstructure and properties in the weld metal and the heat affected zone (HAZ). This cooling rate is determined by a host of different variables such as:

- a) Preheat & interpass temperature
- b) Heat input (including volts, current, wire feed speed, travel speed, contact tip to work distance, and type of waveform)
- c) Power source type & model
- d) Joint design (including groove offset)
- e) Torch configuration (single vs. dual)
- f) Torch spacing
- g) Pass sequence

Of these parameters, heat input is monitored typically as an essential variable because of the effect it has on the thermal cycle and ultimately the mechanical properties of the weld and the heat affected zone. Traditional methods of calculating heat input involve the measuring of either average or root mean square (RMS) voltage and average or RMS current. While not necessarily accurate, this method produces relatively self-consistent results when the welding process used is traditional spray GMAW. The results become less consistent and less accurate with pulse modes due to the rapidly changing output of the machine. True Heat Input has the benefit of rapid enough measurement to accommodate the speed at which the machine operates. To measure the True Heat Input for the weld, it is necessary to determine the True EnergyTM input into the weld. True Energy is The Lincoln Electric Company's technology that involves recording the instantaneous values of the welding output, sampled at a rate of at least 10kHz (10,000 times per

second), to calculate the total amount of power produced during the entire weld. This value is then multiplied by the duration of the weld, to calculate the True Energy (J or kJ) for the weld. Thus, the True Heat Input can be calculated using either of these equations.

$$\text{True Heat Input (J/mm)} = \frac{\text{True Energy (J)}}{\text{Length of Weld (mm)}}$$

or,

$$\text{True Heat Input (J/mm)} = \frac{\text{True Power (W or J/s)} * \text{Time (s)}}{\text{Length of Weld (mm)}}$$

For example, in the first round of 1G welding on X100 pipe, typical differences of 15% - 23% between True Heat Input and Average Heat Input have been observed as reported previously [11, 12].

In this report, the goal has been to identify the primary from the secondary welding variables that have an influence on mechanical properties of the weld and HAZ in mechanized GMAW-P X100 welding.

1.2 Integrated Thermal-Microstructure Model

The first efforts to identify the essential welding variables involved employing an integrated thermal-microstructural model. Details about the development of this model can be found in other topical reports [13, 14] and other publications emanating from this work [15, 16]. Inputs into the model include the groove geometry details, pipe thickness and diameter, shielding gas composition, consumable diameter, welding process parameters for each pass, such as voltage, wire feed speed, current, contact tip to work distance, travel speed, number of passes, torch configuration, and chemical composition of pipe and weld. To simulate the welding process, the thermal model first took the aforementioned inputs and determined the thermal cycles of all welding passes in sequence. These thermal cycles were then fed into the microstructure model to calculate the resulting phase transformations. Subsequently, the final volumetric fractions of different phases, such as ferrite, pearlite, bainite, and martensite, and local hardness throughout the weld metal and its HAZ were determined at the end of the simulation. The integrated thermal-microstructure model can also provide the predicted thermal history at any location in the weld or HAZ.

This model allows virtual experiments to be conducted by varying the aforementioned welding variables to identify the primary and secondary drivers that control thermal behavior, microstructural evolution and ultimately weld and HAZ mechanical behavior.

2 TECHNICAL APPROACH

Significant research has been conducted on development of X100 line pipe and associated welding technology. Previous work [4-8] suggested that control of welding parameters required greater precision than for lower strength pipe grades. This work was undertaken to gain a better understanding of the effect of the essential welding variables on weld quality and properties. Numerous X100 girth pipe welds including 1G rolled single and dual torch welds, 5G single and dual torch welds were completed to understand the effect of various welding variables on the weld and HAZ properties.

One of the major goals of the project was the refinement of numerical models for predicting weld thermal cycles and properties. Ideally, such models would have the capability to accurately calculate the thermal cycles and final hardness in both weld metal and HAZ. The data which would be generated from the full characterization of welding processes, such as welding parameters, temperature and thermal strain histories and post-welding micro-structural study from the experimental welds, was crucial for the verification of these models. In order to generate the necessary data for the model verification and the determination of essential variables, two rounds of girth welding on X100 pipe were undertaken at CRC-EVANS (CRC), while the flat-plate welding was completed at Lincoln Electric. The secondary goal for the project was validation of the final recommendations for essential welding variables and their verification for field conditions. This work was undertaken at CRC and Serimax under Round 3 X100 Pipe welding.

2.1 Design of Experiment (DOE) - Virtual Simulations

A set of virtual experiment simulations were run using the aforementioned model to provide identification of essential welding variables and correlations between essential welding variables and a weld mechanical property such as hardness. Hardness is a fair indicator of the tensile properties of the weld as was observed in results from the first round of 1G welding (Figure 1), where it is evident that higher hardness is associated with higher yield stress (YS) and flow stress (FS) in going from the round tensile bar near the outer diameter of the pipe (OD) to the inner diameter of the pipe (ID) with the strip tensile bar showing properties in between.

Inputs to the model included the following welding variables:

- Preheat and interpass temperature which was varied from 27⁰C to 180⁰C;
- Consumable composition was represented by the carbon equivalent P_{cm} which was varied from 0.25 to 0.33;
- Bevel groove offset distance which was varied from 2.3 mm (0.090 in.) and 2.8 mm (0.110 in.);
- True Heat Input which was varied between 0.35 kJ/mm (9 kJ/in) and 0.71 kJ/mm (18 kJ/in); and
- Torch configuration of single and dual {with 102 mm (4 in.)} spacing torches.

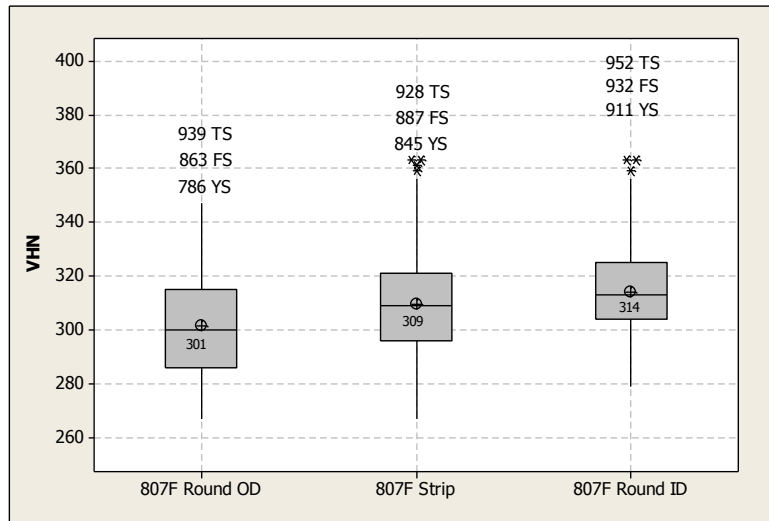


Figure 1. Correlation between the microhardness across the tensile specimen cross section and its average value compared to the 0.2% offset yield (YS), flow stress (FS) and tensile strength (TS) observed in 807F 1G weld from the first round of welding

Groove geometry is illustrated in an earlier report [11]. The number of passes was increased as the groove offset was increased from 2.3 mm (0.090 in.) to 2.8 mm (0.110 in.) and as the True Heat Input was decreased from 0.71 kJ/mm (18 kJ/in.) to 0.35 kJ/mm (9 kJ/in.). The True Heat Input estimate was chosen to be 17% higher than the Average Heat Input. The pipe thickness was fixed at 19.1 mm (0.75 in.) and the pipe composition was also not varied. The gas mixture was selected to be 85% Ar/15% CO₂.

Outputs from the model were:

- Hardness traverse through the centerline of the weld
- 800⁰C to 500⁰C cooling times (t_{85}) and 800⁰C to 400⁰C cooling times (t_{84}) the HAZ adjacent to the 2nd fill pass.

To understand the effects of the different variables, results obtained from the virtual experiments were analyzed statistically using Design-Expert® Software. To simplify the analysis, the mean value of the centerline hardness traverse was utilized as the response indicative of mechanical behavior, because as shown in Figure 1, this value is an indicator of tensile properties. Using analysis of variance, the significance of the input variables in determining mean centerline hardness was ascertained. Details of the virtual experiments are listed in the Appendix.

2.2 Design of Experiment - Plate Welding (DOE)

The results of the virtual experiments provide a basis for conducting welding experiments to experimentally identify the essential variables and validate the predictive capabilities of the model. The primary and secondary variables identified in the virtual simulations were featured in instrumented welding experiments on plate. Simulated pipe joints with flattened X100 pipe material in the flat position were welded using a Fanuc robot coupled with a Power Wave® 455M in a restraining fixture, and voltage, current and HAZ thermal profile were monitored

using high speed data acquisition systems. Twenty-nine simulated pipe joints were welded in the lab using flattened X100 pipe sections, 19.1 mm (0.75 in.) thick, which was left over from the first two rounds of pipe welding. Experimental details are reported by Panday and Daniel [11]. The welding variables were chosen based on the predictions of the virtual model. The True Heat Input range was chosen to encompass the widest range that could be plausibly used in mechanized mainline field GMAW welding of pipe in the 5G position. The consumable composition was expanded to include weld metal P_{cm} values down to 0.21, which is lower than that employed in the virtual simulations. This is because the weld metal Gleeble simulation work [9] showed that the hardness response varies considerably among different weld metal compositions ranging from P_{cm} of 0.21 to 0.28 for 800⁰C to 500⁰C cooling times in the range of 2 to 50 seconds as shown in Figure 2.

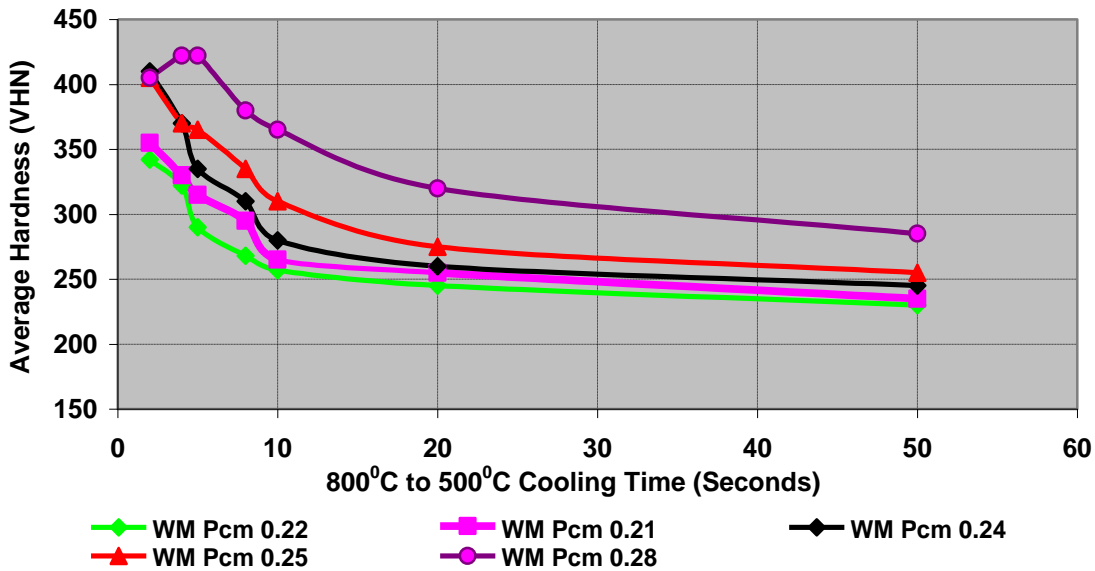


Figure 2. Average Hardness vs. 800⁰C to 500⁰C cooling time from the weld metal Gleeble simulation experiments

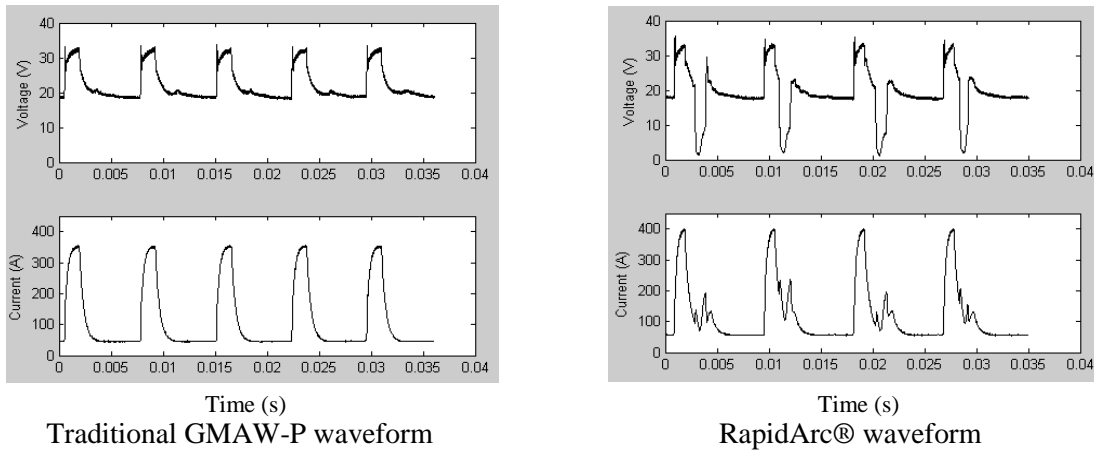
The experimental DOE matrix was determined using a d-optimal design methodology using Design-Expert® software. In d-optimal design, the DOE points are designed to minimize the variance associated with estimates of the model coefficients of the specified model. In this instance, the DOE matrix was designed to capture all linear effects and two factor interaction effects of the following input variables and responses.

The welding input variables were as follows:

- Preheat/Interpass Temperatures selected were 27⁰C, 100⁰C, 180⁰C
- Consumable composition was varied in the range of P_{cm} from 0.22 to 0.33 which resulted in variation in weld metal composition in the range of P_{cm} from 0.21 to 0.32
- Groove Offset varied in the range of 2.3 - 2.8 mm (0.090 - 0.110 in.)
- True Heat Input was varied in the range of 0.46kJ/mm (11.7 kJ/in.) to 0.92 kJ/mm (23.4 kJ/in.) by varying the WFS/TS ratio and using two different pulse waveforms such as traditional pulse and a RapidArc® waveform. These provide nominally different values

of True Heat Input, for the same wire feed speed/travel speed ratio, examples of which are shown in Figure 3. For the entire experimental matrix, the accompanying variation in True Energy/WFS/TS ratio, which is a measure of heat input per unit weld nugget volume, was 0.62-0.89.

- Torch configuration investigated were single torch, dual torch with a 102 mm (4 in.) spacing, and dual torch with a 178 mm (7 in.) spacing
- Gas mixture was fixed at 85%Ar/15%CO₂



For WFS/TS Ratio = 19.1, True Heat Input = 0.47 kJ/mm (12 kJ/in.) For WFS/TS Ratio = 19.1, True Heat Input = 0.55 kJ/mm (14 kJ/in.)
 For WFS/TS Ratio = 26.2, True Heat Input = 0.83 kJ/mm (21 kJ/in.) For WFS/TS Ratio = 26.2, True Heat Input = 0.91 kJ/mm (23 kJ/in.)

Figure 3. Schematic representations of Traditional GMAW-P and RapidArc® waveforms

The responses were:

- Hardness traverse through the centerline of the weld,
- t_{85} (800-500⁰C), t_{84} (800-400⁰C), t_{83} (800-300⁰C) HAZ cooling times (measured at 13.4 mm from bottom of the plate in HAZ location of fill pass 2),
- Tensile properties measured with a strip tensile specimen, and
- Charpy impact toughness over a range of temperatures from 21⁰C, 0⁰C, -20⁰C, -40⁰C, -60⁰C, -80⁰C & -100⁰C

The experimental test matrix is illustrated in Appendix 1.

Statistical methods using analysis of variance was used to determine the significance of the effects of the aforementioned welding input variables on the aforementioned responses. Analysis of variance was used to determine the significance of both linear and interaction effects between the input variables on the aforementioned responses. Transfer functions relating the input variables to the responses were determined and are presented in the results section. These were used to develop recommendations for control of essential variables, the methodology for which is presented in the following section.

2.3 Methodology for the Recommendation of Essential Variables

The methodology for the recommendations utilized the transfer functions to limit the maximum variation in hardness, yield and tensile strengths to $\pm 2\%$ due to variation in the welding input variables. This enabled definition of the envelope of welding input variables such as preheat and interpass temperatures, True Heat Input, and True Heat Input/WFS/TS ratio, which are defined in the results section. WFS/TS ratio is a measure of the volume of weld metal per unit length and needs to be consistent around a nominal value from pass to pass. Otherwise uncontrolled variation would lead to large changes in the weld nugget size which would lead to differences in weld penetration and cooling rate resulting in undesirable variation in mechanical properties. Variation in contact tip to work distance (CTWD) leads to variation in current, which would cause variation in the heat input for the same WFS. Its control within ± 3.2 mm (1/8 in.) provides a feasible approach to reducing the heat input variation. The location of high and low root fitup or misalignment regions of the pipe was recommended to be at the 12 or 6 clock positions because it would be easier to deposit additional weld metal in these positions to compensate for these conditions than at the other clock positions. These recommendations are presented in the section on control of essential variables.

3 RESULTS AND DISCUSSION

3.1 Virtual Experiments

3.1.1 Weld Metal Hardness Predictions

Virtual experiment simulation results were analyzed in the form of box plots of the weld centerline microhardness distribution as well as using statistical methods to predict the dependence of the average weld centerline hardness on the welding variables. Figure 4: Hardness Distributions from Virtual Simulations depicts the one example of the predicted distribution of weld centerline hardness from the simulation.

The number associated with the \oplus symbol represents the average and the number associated with the \otimes symbol represents the median. The box represents the interquartile range (from 25% to 75% of the median) of the distribution. As is evident, the mean hardness increases and the hardness distribution shifts to higher values as the consumable Pcm composition is increased from 0.25 to 0.33 at both 27⁰C and 180⁰C preheat and interpass temperatures at 2.3 mm (0.090 in.) groove offsets. Additionally, at the same Pcm value, increasing the preheat and interpass temperature and the True Heat Input seemed to lower the mean hardness and the hardness distribution.

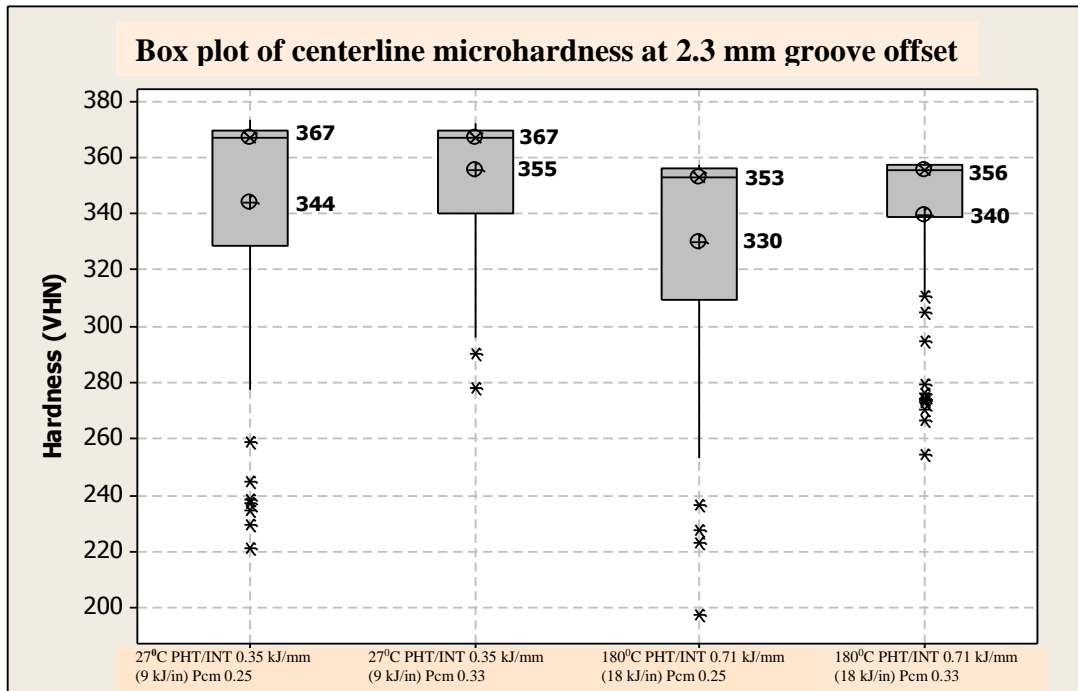


Figure 4: Hardness Distributions from Virtual Simulations

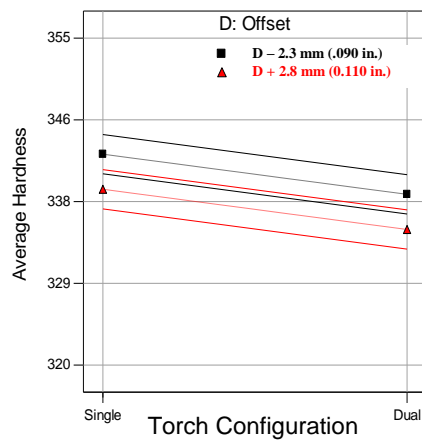


Figure 5: Effect of joint offset and torch configuration on average centerline weld hardness True Heat Input= 0.53 kJ/mm (13.5 kJ/in.), Pcm=0.29, PHT/INT=104

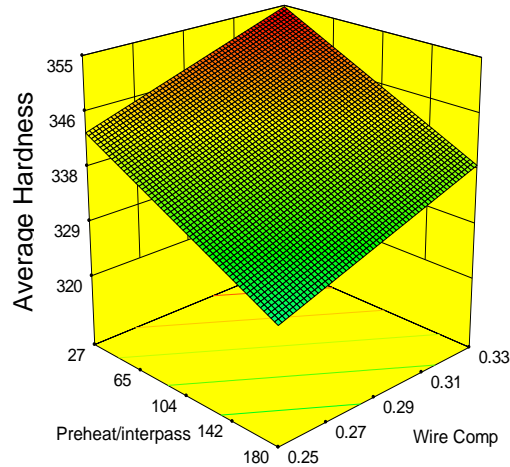


Figure 6: Effect of preheat / interpass and consumable composition, Pcm, on average centerline weld hardness True Heat Input= 0.53 kJ/mm (13.5 kJ/in.), Offset=0.10, Single Torch

Results of statistical analysis using Design-Expert are presented in Figure 5 and Figure 6. The preheat and interpass temperatures and consumable composition are predicted to be the primary variables that affect weld metal hardness. As the preheat and interpass temperature increased from 27⁰C to 180⁰C and the consumable carbon equivalent Pcm is decreased from 0.33 to 0.25, the weld hardness decreases quite significantly. The groove offset and the torch configurations are identified as the secondary variables in their effect on weld hardness. As the groove offset is increased from 2.3 mm (0.090 in.) to 2.8 mm (0.110 in.) and the torch configuration is increased from single to dual, the hardness decreases, but the effect is smaller than with the primary variables. Results of the analysis of variance are presented in the appendix. These effects are consistent with observations in earlier studies. True Heat Input was not predicted as a significant factor affecting hardness. This prediction is counter intuitive and not consistent with what has been observed in earlier studies. There could be a couple of reasons why True Heat Input was not predicted as a significant variable that affects hardness. One reason could be that even as the True Heat Input was varied, the True Heat Input/WFS/TS ratio which is a measure of heat input per unit weld nugget volume is estimated to have not changed significantly in the virtual experiment as shown in Appendix 1. The other reason could be that the integrated thermal microstructural model requires refinement of its hardness prediction. This model, however, does recognize True Heat Input as a significant factor that provides cooling rate predictions that are closer to experimental results (compared to that based on average heat input) as shown in Figure 7. This is because the true heat input is 15%-23% higher than heat input based on average values of voltage and current in the pulse programs used in this study [11,12]. In any case, it seems that the link between the cooling rate and hardness presumably requires more refinement to capture the effect of True Heat Input on hardness.

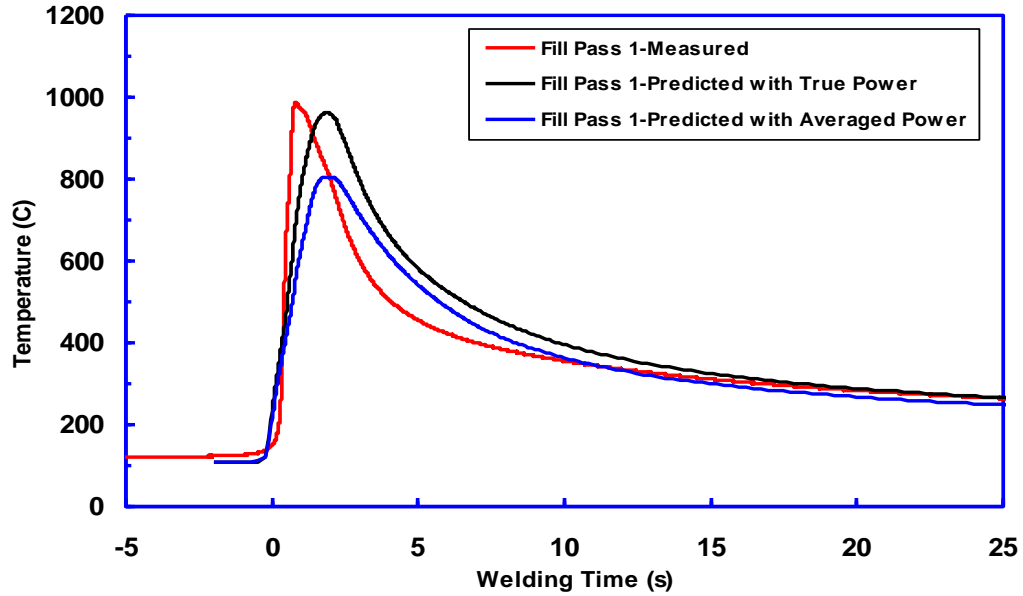


Figure 7. HAZ t₈₅ cooling predictions with true and average heat input compared to experimental results

3.1.2 HAZ Cooling Time Predictions

Results of the cooling time predictions are presented in Figure 8 and Figure 9. Preheat and interpass temperatures and True Heat Input are predicted to be the primary variables that affect the HAZ t₈₅ cooling times. As these variables are increased, the HAZ t₈₅ cooling times increase dramatically. The groove offset was identified as a secondary variable in that increasing the offset caused a smaller increase in the HAZ t₈₅ cooling times. These trends are once again consistent with what has been observed with earlier experiments.

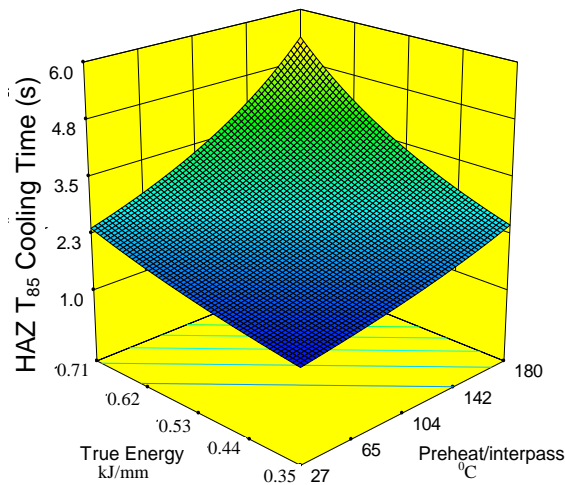


Figure 8: : Effect of preheat / interpass temperatures and True Heat Input on HAZ t₈₅ cooling times

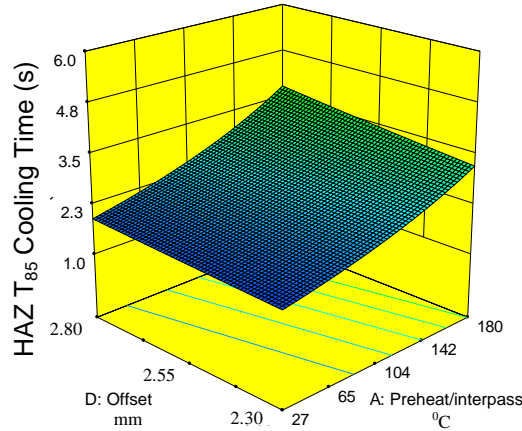


Figure 9: Effect of preheat / interpass temperatures and groove offset on HAZ t₈₅ cooling times

3.2 Plate Experiment Results

Statistical analysis of the results indicate that a linear model can be fit between the welding variables and the responses such as average weld centerline hardness, yield strength, tensile strength, Charpy impact toughness at -20°C and the HAZ t_{85} , t_{84} , t_{83} cooling times.

The welding variables that affect hardness, tensile strength and yield strength are preheat and interpass temperatures, weld composition, True Heat Input and torch configuration. Groove offset was not seen to be a controlling variable. The R^2 of the linear model is 96%, 96% and 86% with hardness, tensile strength and yield strength respectively, indicating a very good fit. In the statistical analysis, the True Heat Input (HI_{TE}) and the True Heat Input (HI_{TE})/WFS/TS ratio are interrelated variables and only one of them can be analyzed at any given time. Since their effects on the responses were similar, True Heat Input was used in all the statistical analysis in place of the (HI_{TE})/WFS/TS ratio for clarity. However, knowing the HI_{TE} and WFS/TS, this ratio can be derived at any time for control purposes.

The variables that affect the t_{85} , t_{84} , t_{83} cooling times in the HAZ are preheat and interpass temperature, True Heat Input, and torch configuration, whereas groove offset and weld composition do not have any influence. The predicted R^2 of the linear model featuring these responses is about 98% which indicates excellent fit between these variables and the HAZ cooling times.

The variables that affect the Charpy impact toughness are preheat and interpass temperature, weld composition and torch configuration, whereas True Heat Input and groove offset are not seen as significant variables. The predicted R^2 of the linear model featuring this response is 49%, indicating that a higher degree of scatter is associated with the Charpy toughness measurement. Transfer functions that correlate the effects of the aforementioned input variables on the aforementioned responses have been obtained from the statistical analysis, and these are listed in Table 1. The magnitude of these transfer functions and the resulting trends of the responses as a functions of the welding input variables are in accordance with fundamental principles regarding their effects. This has allowed quantification of their effects on narrow gap X100 welds. The following discussion provides graphical illustration of these effects.

Figures 10 through 12 illustrate the influence of the welding variables on average weld centerline hardness. As is evident, the weld composition has the largest influence, followed by preheat and interpass temperature followed by True Heat Input with the weld hardness increasing with increasing weld alloy composition represented by Pcm, decreasing preheat and interpass temperatures and True Heat Input. Also, the hardness drops noticeably when the torch configuration is changed from a single to a dual torch with 178 mm (7 in.) torch spacing and decreases further when the spacing between the torches is decreased to 102 mm (4 in.)

Table 1. Transfer Functions from DOE Plate Welds

Torch Configuration- Single Torch			
Average Center Line Hardness (VHN) =	166 - 0.23*Preheat/IPT	+ 882*Weld Composition (Pcm)	- 51*True Heat Input
Yield Strength (MPa) =	444 - 0.65*Preheat/IPT	+ 2526*Weld Composition (Pcm)	- 217*True Heat Input
Tensile Strength (MPa) =	332 - 0.63*Preheat/IPT	+ 3300*Weld Composition (Pcm)	- 148*True Heat Input
CVN Toughness @-20°C (J) =	234 + 0.33*Preheat/IPT	- 544*Weld Composition (Pcm)	
HAZ FP2* Cooling Time Ln(t ₈₅) (s) =	-0.96 + 0.005*Preheat/IPT	+ 2.3*True Heat Input	
HAZ FP2* Cooling Time Ln(t ₈₄) (s) =	-0.39 + 6.95*Preheat/IPT	+ 2.3*True Heat Input	
HAZ FP2* Cooling Time Ln(t ₈₃) (s) =	0.34 + 9.66*Preheat/IPT	+ 2.2*True Heat Input	
Torch Configuration- Dual Torch 178 mm (7") Gap			
Average Center Line Hardness (VHN) =	142 - 0.23*Preheat/IPT	+ 882*Weld Composition (Pcm)	- 51*True Heat Input
Yield Strength (MPa) =	365 - 0.65*Preheat/IPT	+ 2526*Weld Composition (Pcm)	- 217*True Heat Input
Tensile Strength (MPa) =	244 - 0.63*Preheat/IPT	+ 3300*Weld Composition (Pcm)	- 148*True Heat Input
CVN Toughness @-20°C (J) =	266 + 0.33*Preheat/IPT	- 544*Weld Composition (Pcm)	
HAZ FP2* Cooling Time Ln(t ₈₅) (s) =	-0.41 + 0.005*Preheat/IPT	+ 2.3*True Heat Input	
HAZ FP2* Cooling Time Ln(t ₈₄) (s) =	0.28 + 6.95*Preheat/IPT	+ 2.3*True Heat Input	
HAZ FP2* Cooling Time Ln(t ₈₃) (s) =	1.02 + 9.66*Preheat/IPT	+ 2.2*True Heat Input	
Torch Configuration- Dual Torch 100 mm (4") Gap			
Average Center Line Hardness (VHN) =	135 - 0.23*Preheat/IPT	+ 882*Weld Composition (Pcm)	- 51*True Heat Input
Yield Strength (MPa) =	341 - 0.65*Preheat/IPT	+ 2526*Weld Composition (Pcm)	- 217*True Heat Input
Tensile Strength (MPa) =	211 - 0.63*Preheat/IPT	+ 3300*Weld Composition (Pcm)	- 148*True Heat Input
CVN Toughness @-20°C (J) =	274 + 0.33*Preheat/IPT	- 544*Weld Composition (Pcm)	
HAZ FP2* Cooling Time Ln(t ₈₅) (s) =	-0.15 + 0.005*Preheat/IPT	+ 2.3*True Heat Input	
HAZ FP2* Cooling Time Ln(t ₈₄) (s) =	0.51 + 6.95*Preheat/IPT	+ 2.3*True Heat Input	
HAZ FP2* Cooling Time Ln(t ₈₃) (s) =	1.14 + 9.66*Preheat/IPT	+ 2.2*True Heat Input	

*FP2 = Fill Pass 2

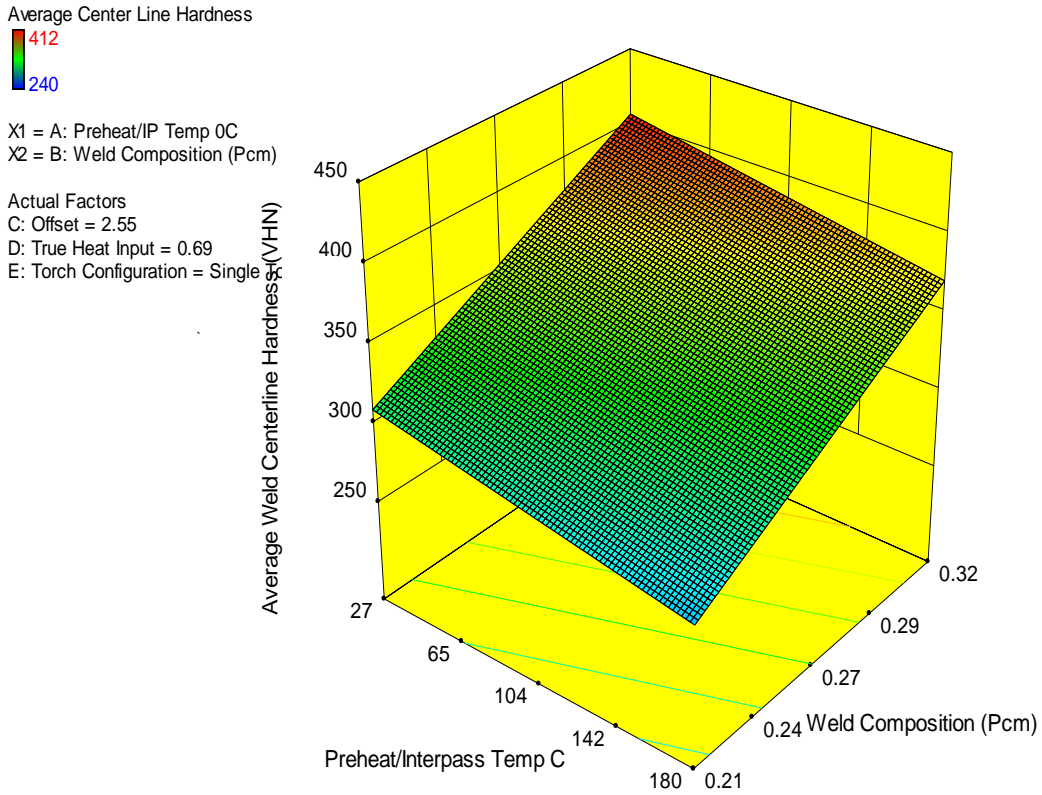


Figure 10. Effect of Preheat/Interpass Temperature and Weld Composition on Average Weld Centerline Hardness

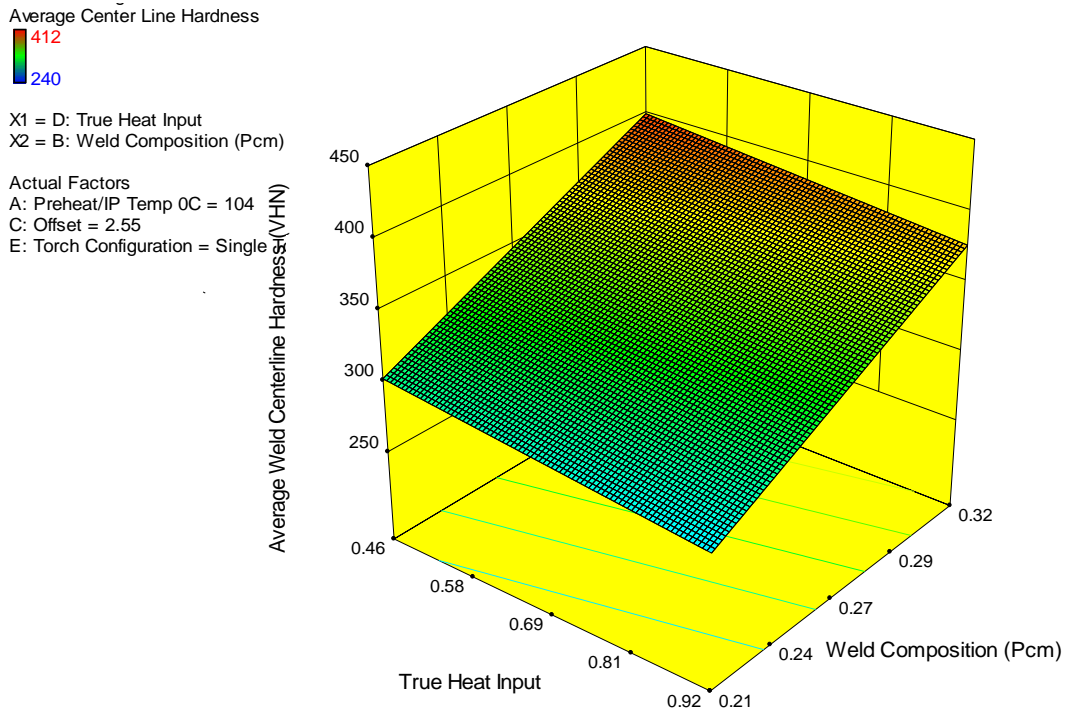


Figure 11. Effect of True Heat Input and Weld Composition on Average Weld Centerline Hardness

Factor: Welding Process
 Average Center Line Hardness

X1 = E: Torch Configuration
 X2 = B: Weld Composition (Pcm)

Actual Factors
 A: Preheat/IP Temp 0C = 104
 C: Offset = 2.55
 D: True Heat Input = 0.69

■ B- 0.21
 ▲ B+ 0.32

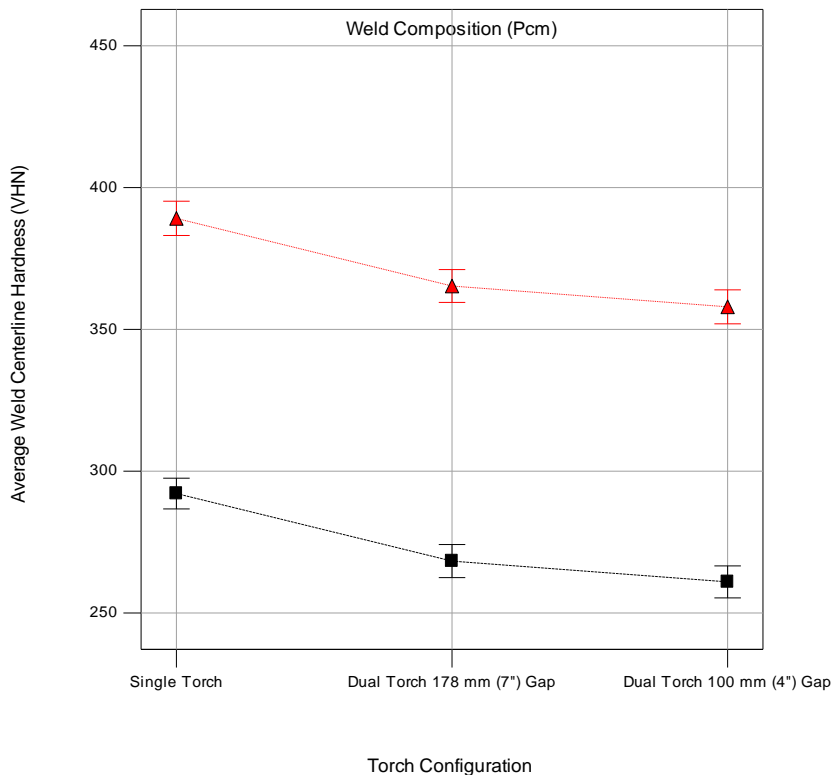


Figure 12. Effect of Torch configuration and Weld Composition on Average Weld Centerline Hardness

The influence of the welding variables on weld tensile and yield strength is similar in nature to that observed with the hardness as shown in Figures 13 through 15, and 16 through 18. Weld composition has the most influence on tensile and yield strengths and followed by preheat and interpass temperature and True Heat Input. The impact of torch configuration is similar to that observed with hardness whereby the single torch provides the highest tensile and yield strengths followed by the dual torch with a 178 mm (7 in.) spacing and the dual torch with a 102 mm (4 in.) spacing.

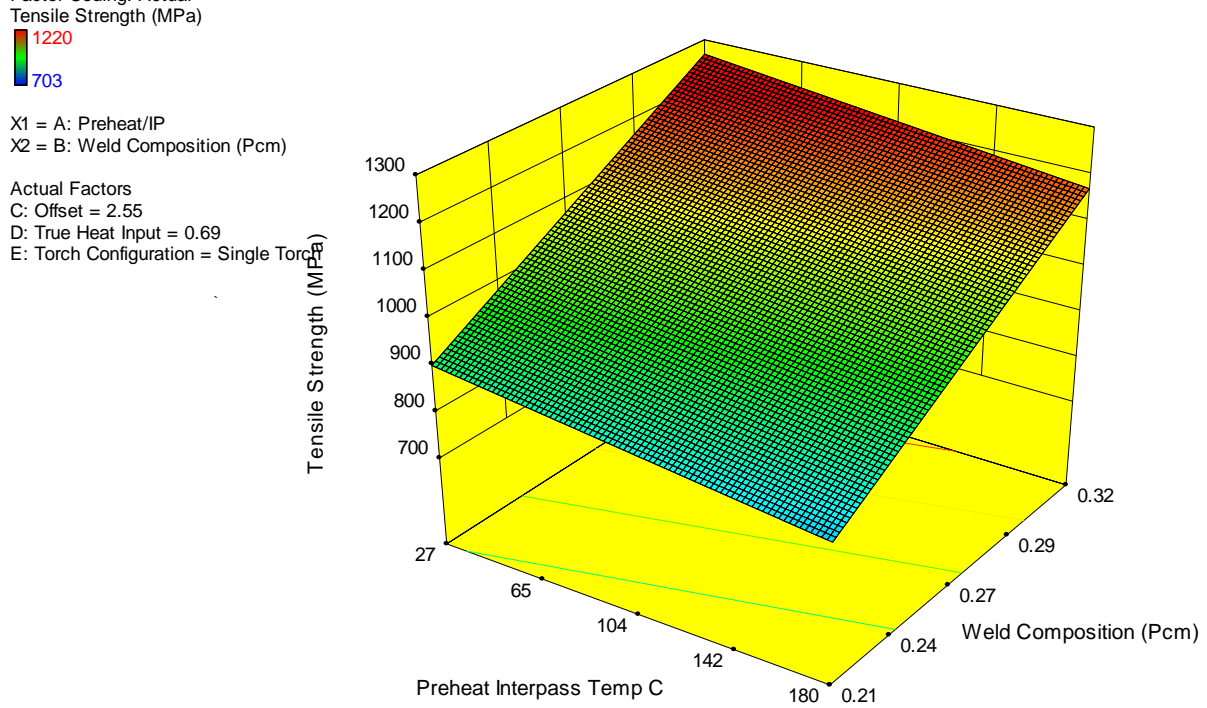


Figure 13. Effect of Preheat/Interpass and Composition on Weld Tensile Strength

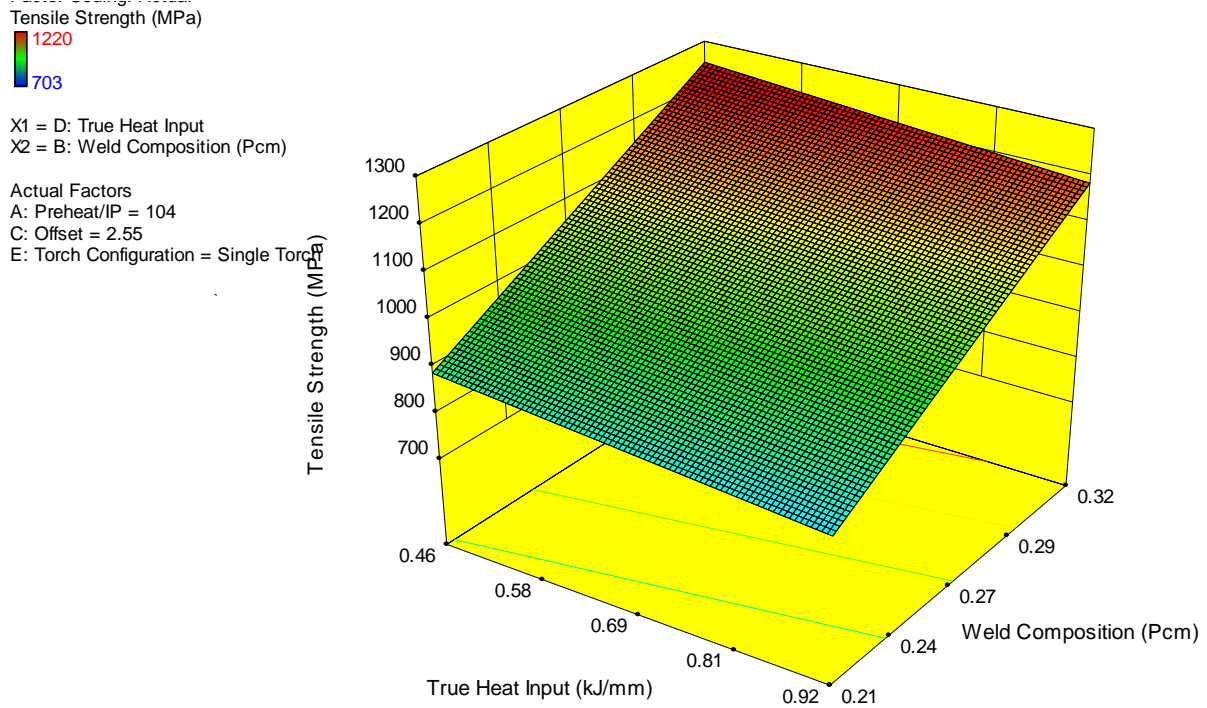


Figure 14. Effect of True Heat Input and Composition on Weld Tensile Strength

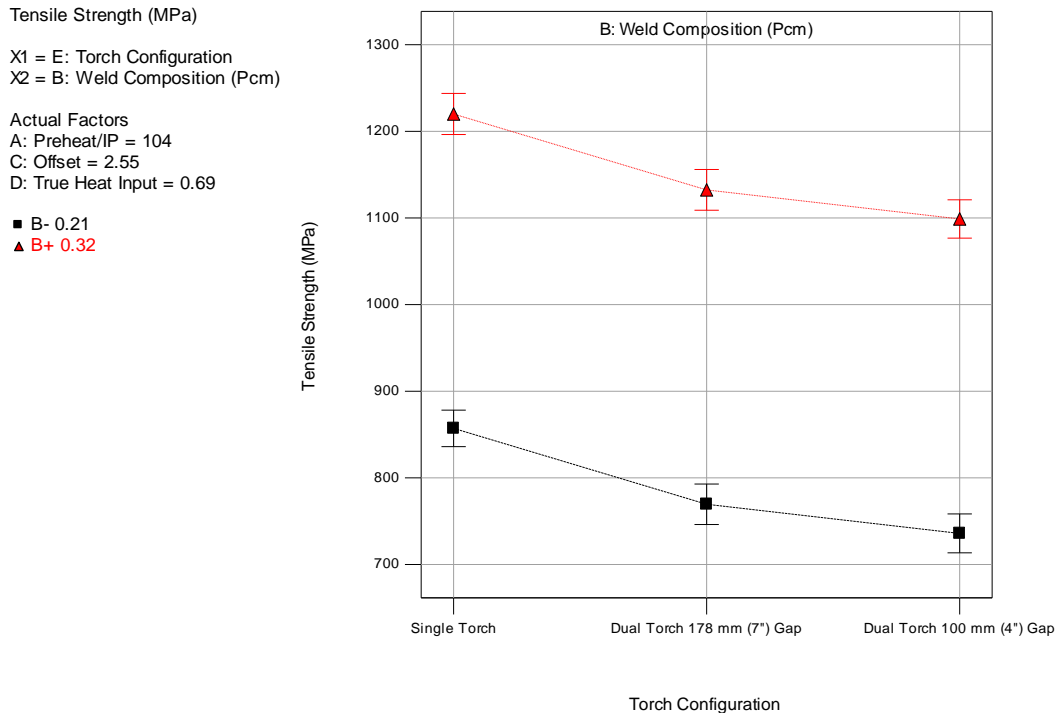


Figure 15. Effect of Torch configuration and Weld Composition on Weld Tensile Strength

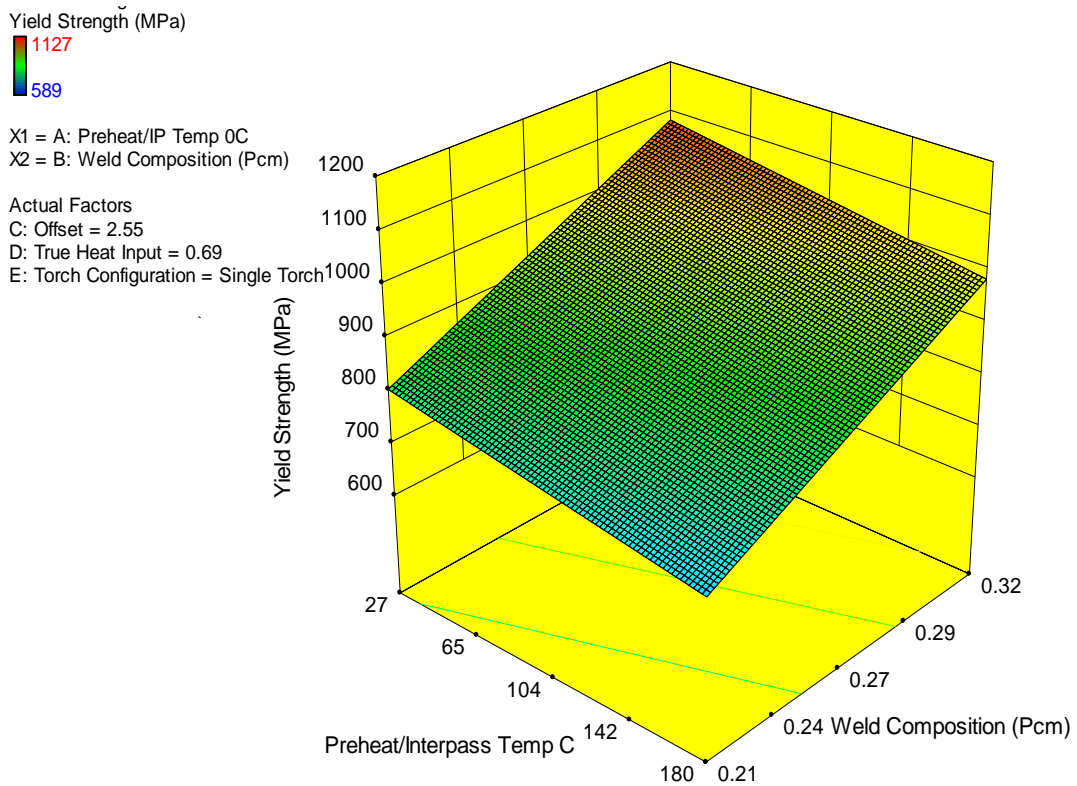


Figure 16. Effect of Preheat/Interpass Temperature and Weld Composition on Weld Yield Strength

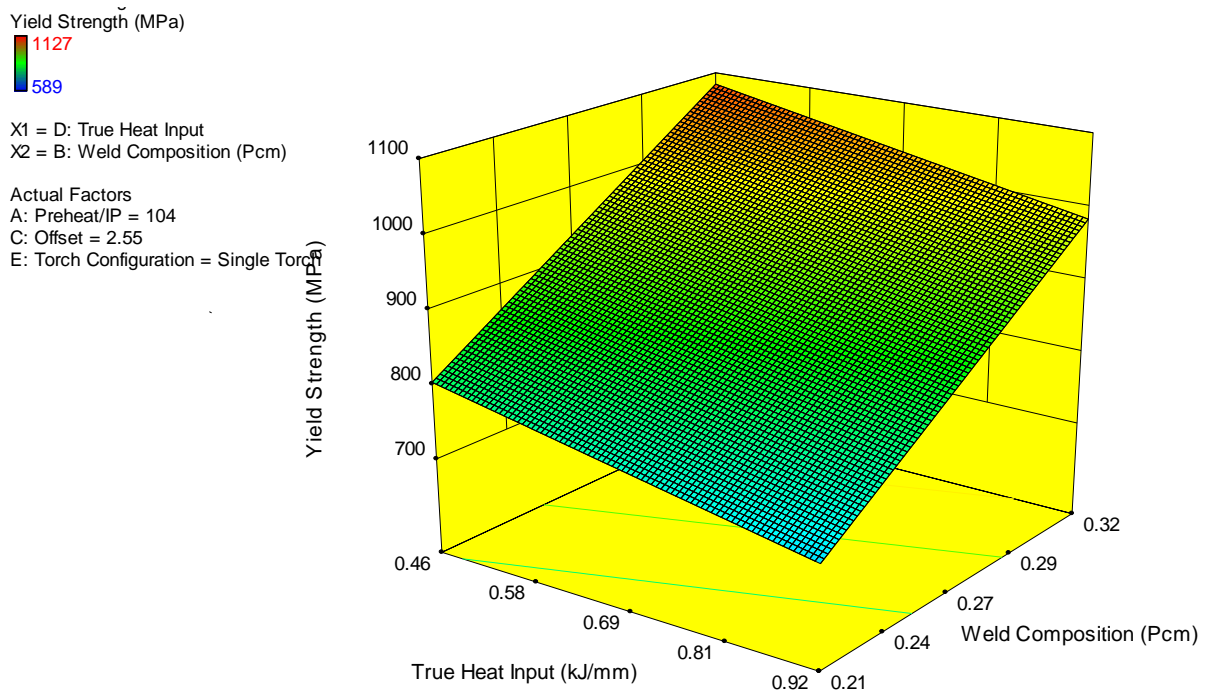


Figure 17. Effect of True Heat Input and Composition on Weld Yield Strength

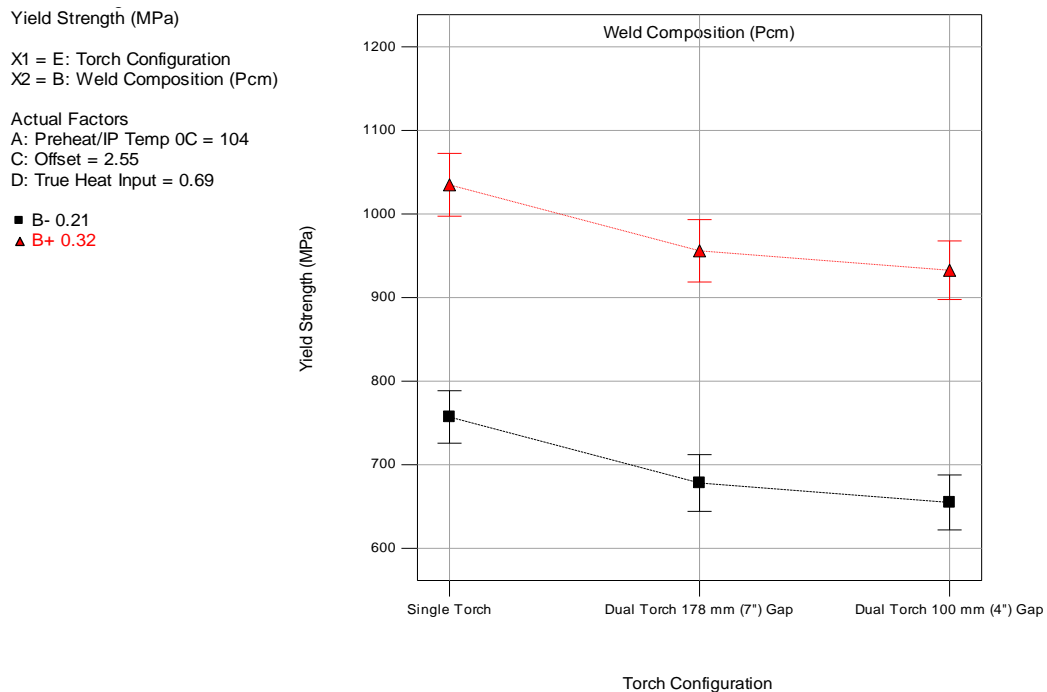


Figure 18. Effect of Torch configuration and Weld Composition on Weld Yield Strength

The t_{85} (800-500⁰C), t_{84} (800-400⁰C), t_{83} (800-300⁰C) HAZ cooling times increase significantly with increasing preheat and interpass temperature and increasing True Heat Input. The trend of t_{85} HAZ cooling times with preheat and interpass temperature and true heat input is shown in Figure 19. The t_{85} HAZ cooling time increases from 1.5 to 3.5 seconds with an increase in true

heat input from 0.46 kJ/mm (11.7 kJ/in.) to 0.92 kJ/mm (23.4 kJ/in) at 27⁰C interpass temperature, and increases from 1.5 to 2.5 seconds with an increase in interpass temperature from 27⁰C to 180⁰C at 0.46 kJ/mm, but the increase is more dramatic to about 8 seconds with the cumulative effect of higher heat input (0.92 kJ/mm) and interpass temperature (180⁰C). This trend agrees very well with the trend from the thermal model predictions shown earlier in Figure 8. The trends observed with the t₈₄ and t₈₃ HAZ cooling times were very similar except the magnitudes of cooling times were much higher.

The change from a single to a dual torch has a dramatic effect in increasing the t₈₅ HAZ cooling times. The change in torch spacing from a single to dual torch with 102 mm (4 in.) spacing causes the t₈₅ HAZ cooling time to increase from about 2 seconds at 0.46 kJ/mm to about 12 seconds at 0.92 kJ/mm at 104⁰C Preheat/Interpass temperature as shown in Figure 20. At higher preheat and interpass temperatures of 180⁰C, the t₈₅ HAZ cooling times increased to about 18 seconds at the highest inputs (0.92 kJ/mm). The strong dependence of the HAZ cooling times with the welding process parameters highlights their potential impact on the transformation characteristics and subsequent development of mechanical properties in the HAZ.

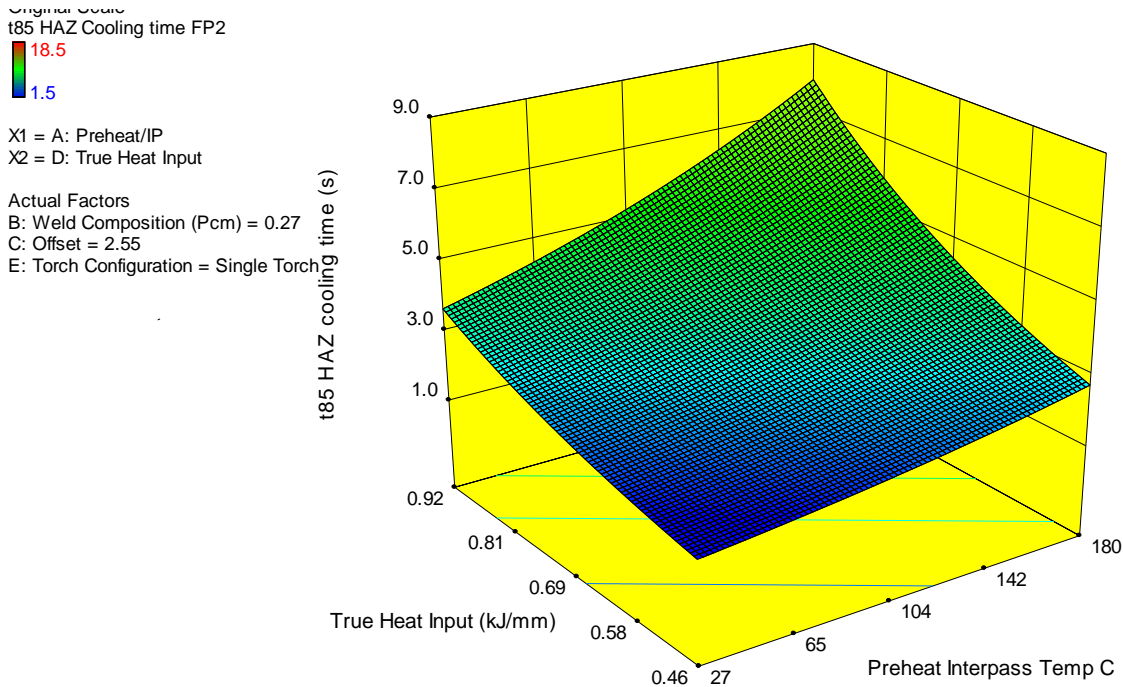


Figure 19. Effect of Preheat/Interpass Temperature and True Heat Input on t85 cooling times in the HAZ near fill pass 2.

Original Scale
t85 HAZ Cooling time FP2

X1 = E: Torch Configuration
X2 = D: True Heat Input

Actual Factors

A: Preheat/IP = 104
B: Weld Composition (Pcm) = 0.27
C: Offset = 2.55

■ D- 0.46
▲ D+ 0.92

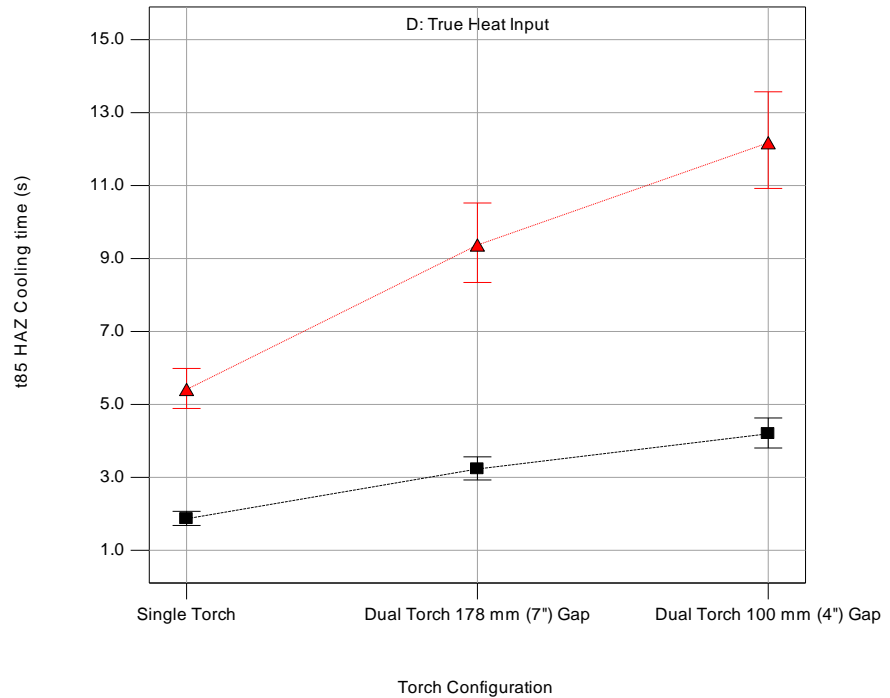


Figure 20. Effect of Torch configuration and preheat and interpass temperature on t85 cooling times in the HAZ near fill pass 2.

Leaner weld metal compositions and higher preheat and interpass temperatures lead to higher Charpy toughness as shown in Figure 21. Also, dual torch with 102 mm (4 in.) spacing provides the highest toughness whereas the single torch provides the least toughness with the dual torch with the 178 mm (7 in.) spacing providing intermediate values of toughness as shown in Figure 22. The effect of these variables on toughness is understandably exactly opposite of their effect on strength.

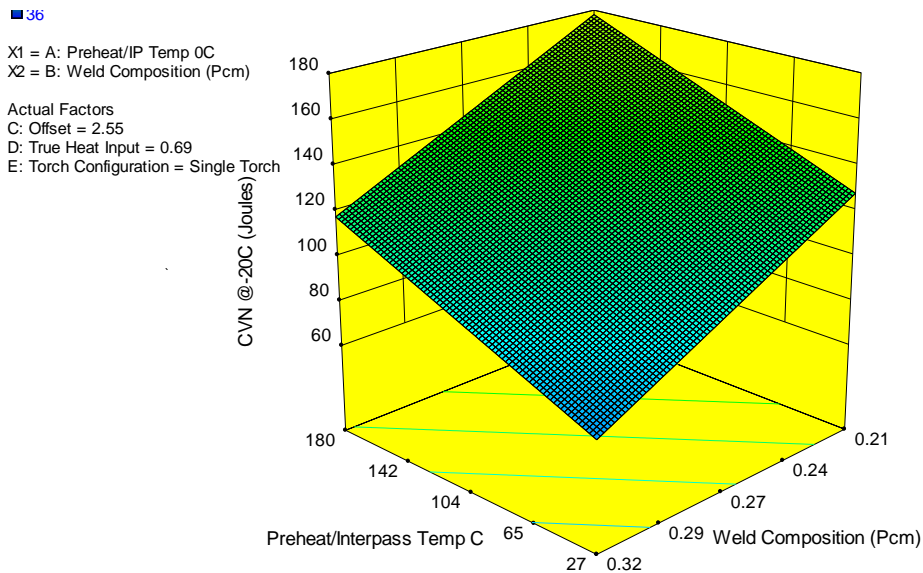


Figure 21. Effect of Preheat/Interpass Temperature and True Heat Input on Charpy Impact Toughness at -20°C

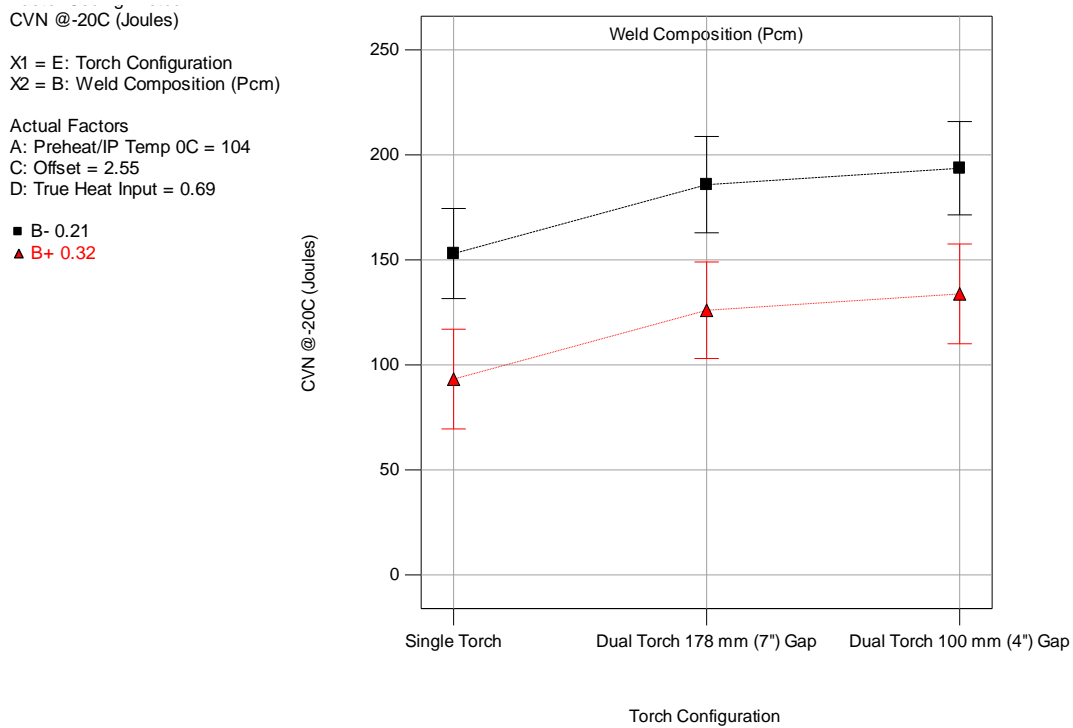


Figure 22. Effect of Torch configuration and Weld Composition on Charpy Impact Toughness at -20°C

3.3 Control of Essential Variables

As mentioned in the preceding section on results, development of the statistical models relating the welding variables to weld properties has enabled the development of transfer functions shown earlier in Table 1. These transfer functions can now be utilized to determine the control necessary in the welding process variables to reduce variation in weld mechanical properties. Also, these transfer functions can be used to generate optimization graphs for desired yield and tensile strength limits in preheat and interpass temperature vs. True Heat Input space for a given torch configuration and weld composition. This methodology for procedure control is illustrated via the example shown in Figure 23, where for a single torch weld with a composition of 0.22 Pcm, the envelope of welding variables is defined for a yield strength range of 795-830 MPa (115-120 ksi), tensile strength range of 895-940 (130-136 ksi), and a mean weld metal centerline hardness range of 302-315 VHN. These ranges represent a $\pm 2\%$ variation in each of these properties around their mean value that was mentioned in the Technical Approach section. For a preheat/interpass temperature of about 100°C, the allowable True Heat Input range is between 0.55 - 0.71 kJ/mm (14 -18 kJ/in), and for 125°C, the allowable True Heat Input range is 0.47 - 0.63 kJ/mm (12-16 kJ/in). If the preheat and interpass temperature varies between 100°C and 125°C, then the allowable True Heat Input range decreases to 0.55 - 0.63 kJ/mm (14-16 kJ/in) as shown by the rectangular block in Figure 23. Keeping the true heat input variation within ± 0.08 kJ/mm (± 2 kJ/in) for a given preheat and interpass temperature would allow the mechanical property variation to be within $\pm 2\%$ of a nominal value.

DesignExpert Software
Overlay Plot

Average Center Line Hardness
Yield Strength MPa
Tensile Strength MPa

X1 = D: True Heat Input
X2 = A: Preheat/IP

Actual Factors
B: Weld Composition (Pcm) = 0.22
C: Offset = 2.55 mm
E: Torch Configuration = Single Torch

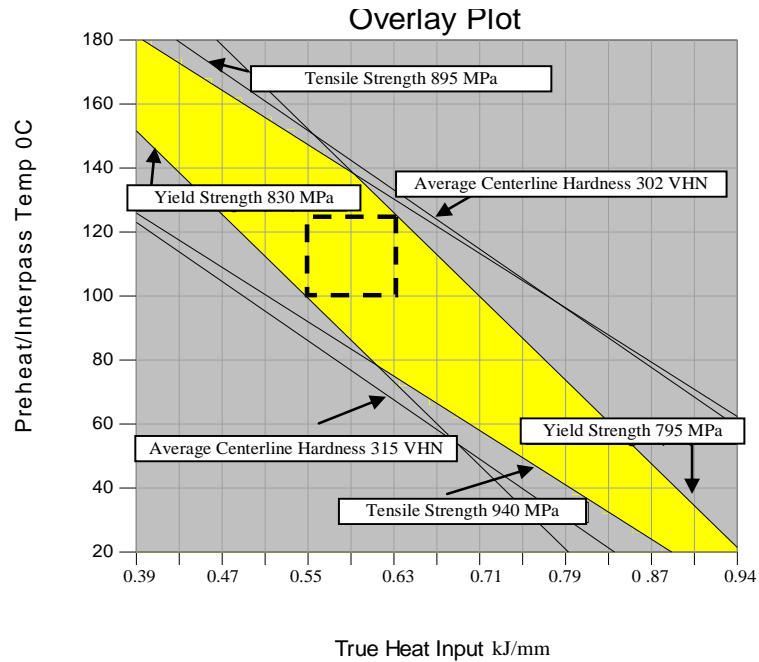


Figure 23. Optimization graph relating yield and tensile strength to preheat/interpass temperatures and True Heat Input values for a single torch weld with a composition indicated by Pcm=0.22

Using this approach, recommendations for control of the essential variables have been outlined. These recommended controls were used by contractors to fabricate welds in their facilities under field welding conditions. They are as follows:

- Preheat and interpass temperatures to be maintained at $100^{\circ}\text{C} +15^{\circ}\text{C} -0^{\circ}\text{C}$. Temperature to be measured at 12, 3, 6 and 9 clock positions around the pipe
- Wire feed speed (WFS)/Travel Speed (TS) ratio to be maintained as consistent as possible for all fill passes. For the final fill passes, TS could vary as much as 15% or WFS could vary as much as 10% from nominal settings.
- Heat input (HI) is to be based on True Energy continuously and maintained at ± 0.08 kJ/mm (± 2 kJ/in) for all fill passes.
- HI/(WFS/TS ratio) tolerance of ± 0.04 for all passes
- Contact tip to work distance to be maintained at ± 3.2 mm ($\pm 1/8$ in.) for all passes.
- Groove offset tolerance of ± 0.3 mm (± 0.01 in.)
- Preferred location for any high/low root fit up condition should be at 12 or 6 clock position

3.4 Application of Essential Variable Control to Field Welding Conditions

To implement essential variable control in field welding, two contractors A and B were selected to conduct 5G welding on X100 pipe and asked to control the welding process within the recommended limits for essential welding variables. This welding effort is referred to as the third round of welding [11]. The pipe selected for the welding was 1067 mm (42 in.) diameter with 14-15 mm nominal wall thickness. Both single and dual torch girth welds were made on the pipe. Both contractors used their own power sources, joint geometries, weld schedules, gas mixtures and torch spacing configurations. In this report, only the single torch welding will be

discussed. Results of dual torch welding from these initiatives are reported by Rajan and Daniel [17]. Details of the welding procedures are listed in Table 2.

Table 2. Pipe Welding Procedures Under Field Welding Conditions

Welds made by Contractor A								
Weld ID	Pipe	Torch Configuration	Waveform	Gas	Preheat Temp °C	Interpass Temp °C	Consumable	Consumable Pcm
952-D	A	Single	Pulse	85%Ar/15%CO ₂	100-125	100-125	PT1	0.28
952-F	B	Single	Pulse	85%Ar/15%CO ₂	100-125	100-125	PT1	0.28
Welds made by Contractor B								
Weld 3	A	Single	Constant Voltage	50%Ar/50%CO ₂	100-130	100-140	PT1	0.28
Weld 4	B	Single	Constant Voltage	50%Ar/50%CO ₂	100-130	105-140	PT1	0.28

X100 pipes 1067 mm (42 in.) in diameter with 14-15 mm nominal wall thickness from two different sources identified as Pipe A and Pipe B with different compositions were employed. Details of the pipe composition and properties are listed in the Appendix.

Measurement of the True Energy for the welds revealed that the difference between True Heat Input and Average Heat Input with contractor A was 18-22% in the fill passes and about 23% in the cap passes, whereas with contractor B the difference between them was negligible. This is reflective of the fact that contractor A used a pulse waveform and contractor B used a constant voltage process in the globular/shorting mode. These differences highlight the importance of recording True Energy such that the True Heat Input can be measured irrespective of the nature of the waveform that will be used. No significant differences were observed in the preheat and interpass temperatures utilized by the different contractors.

The variation of True Heat Input was analyzed as a function of clock position for each pass as opposed to just looking at the composite True Heat Input for the pass. This was done because data from the 5G welds from the second round of welding had indicated that significant variation in heat input can be encountered in each pass. This is because changes are made to the welding procedures at the different clock positions as part of conventional practice to control the weld puddle to provide sound weld metal. Analysis and reporting of the True Heat Input as a function of clock position allows identification of the extent of this variation, such that tighter control can be implemented in field practice.

The variation of True Heat Input as a function of clock position with the contractor A, revealed that there were several instances where the True Heat Input varied more than ± 0.08 kJ/mm (2 kJ/in) around the clock position. One example of such variation is shown in Figure 24 where the heat input varied from 0.8 kJ/mm (20 kJ/in) to 0.6 kJ/mm (15 kJ/in) in going from the 12 to 3 clock position and then back to 0.8 kJ/mm (20 kJ/in) from 4:30 to 6 clock positions. The

magnitude of this variation was not consistent from pass to pass even though the contractor used his own procedures and methods.

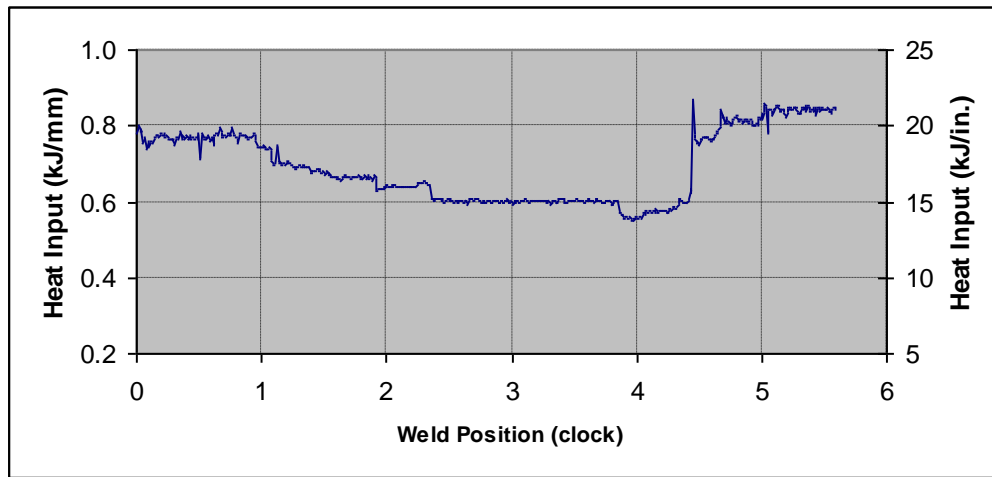


Figure 24. Variation of True Heat Input with clock position, Weld 952-D fill pass 2

Results of the True Heat input values obtained from welds 952-D and 952-F with contractor A indicating the extent of the variation are shown in Tables 3 and 4. In fill pass 2, the True Heat Input varied as a function of clock position from 0.77 kJ/mm (20 kJ/in) at 12 clock to 0.6 kJ/mm (15 kJ/in) at 3 clock and back to 0.84 kJ/mm (21 kJ/in.) at the 6 clock position. In fill pass 3, the true heat input varies from about 0.63 kJ/mm (16 kJ/in.) at the 12 and 3 clock positions to about 0.77 kJ/mm (20 kJ/in.) at the 6 clock position. At a given clock position, the heat inputs varied from 0.75 kJ/mm (19 kJ/in.) in fill pass 1 to 0.6-0.62 kJ/mm (15-16 kJ/in.) in fill passes 2 and 3 in the 3 clock position, from 0.76-0.77 kJ/mm (19.5 kJ/in.) in fill pass 1 and 2 to 0.63 kJ/mm (16 kJ/in.) in fill pass 3 at the 12 clock position. In the 6 clock position, the heat input stayed nominally at 0.77-0.84 kJ/mm (20-21 kJ/in.) in the fill passes.

Table 3. True Heat Input values (kJ/mm) in weld 952-D

							Average Fill Pass 1 to 3	Standard Deviation Fill Pass 1 to 3
Clock Position	Hot Pass	Fill Pass 1	Fill Pass 2	Fill Pass 3	Cap 1	Cap 2	FP1-3	FP1-3
12 o'clock	0.31	0.76	0.77	0.63	0.56	0.61	0.72	0.08
3 o'clock	0.31	0.75	0.60	0.62	0.51	0.50	0.66	0.08
6 o'clock	0.30	0.80	0.84	0.77	0.66	0.61	0.80	0.04

Table 4. True Heat Input values (kJ/mm) in weld 952-F

							Average Fill Pass 1 to 3	Standard Deviation Fill Pass 1 to 3
Clock Position	Hot Pass	Fill Pass 1	Fill Pass 2	Fill Pass 3	Cap 1	Cap 2	FP1-3	FP1-3
12 o'clock	0.31	0.76	0.77	0.76	0.59	0.61	0.77	0.01
3 o'clock	0.31	0.76	0.60	0.61	0.50	0.49	0.66	0.09
6 o'clock	0.30	0.80	0.83	0.77	0.71	0.70	0.80	0.03

With contractor B, most of the variation was in the 12-1 clock position after which the True Heat Input was in a fairly tight range. Typical example of this is shown in Figure 25. Results of the True Heat input values obtained from welds 3 and 4 with contractor B are shown in Tables 5 and 6. In this instance, in a given fill pass, the variation around the clock position was much smaller. In fill pass 1-3, the True Heat Input varied from about 0.56-0.6 kJ/mm (14 - 15 kJ/in.) at the 12 clock position to about 0.46-0.51 kJ/mm (12-13 kJ/in) in the 3 clock position and 0.55 kJ/mm (14 kJ/in.) in the 6 clock position. In fill pass 4, heat input at the 3 clock position was lowered to about 0.44 kJ/mm (11 kJ/in.). At a given clock position, the heat input in each pass was consistent and was around 0.55-0.57 kJ/mm (14-14.5 kJ/in.) at the 12 clock position, 0.44-0.51 kJ/mm (11-13 kJ/in.) at the 3 clock position and 0.55-0.6 kJ/mm (14-15kJ/in.) for weld 3 and 0.49-0.57 kJ/mm (12.4 -14.5 kJ/in.) for weld 4 at the 6 clock position. In general, the heat input variation in a pass and from pass to pass was much lower than with contractor A.

Small scale tests were conducted in the clock positions of 12-1, 2:30-3:30, and 5-6 clock positions and these are referred to nominally as 12, 3 and 6 clock positions. Small scale tests reported here include strip tensile tests and Charpy impact toughness results.

Table 5. True Heat Input values (kJ/in) in weld 3

Clock Position	Root	Hot Pass	Fill Pass 1	Fill Pass 2	Fill Pass 3	Fill Pass 4	Strip Pass Fill 4	Cap 1	Cap 2	Average Fill Pass 1 to 4	Standard Deviation Fill Pass 1 to 4
12 o'clock	0.37	0.61	0.58	0.61	0.56	0.57		0.46	0.52	0.58	0.03
3 o'clock	0.28	0.50	0.49	0.51	0.51	0.44	0.46	0.39	0.43	0.48	0.03
6 o'clock	0.38	0.57	0.55	0.57	0.55	0.57		0.59	0.68	0.56	0.01

Table 6. True Heat Input values (kJ/in) in weld 4

Clock Position	Root	Hot Pass	Fill Pass 1	Fill Pass 2	Fill Pass 3	Fill Pass 4	Strip Pass Fill 4	Cap 1	Cap 2	Average Fill Pass 1 to 4	Standard Deviation Fill Pass 1 to 4
12 o'clock	0.37	0.61	0.61	0.60	0.59	0.58	0.58	0.52	0.52	0.59	0.01
3 o'clock	0.31	0.49	0.49	0.49	0.46	0.44		0.42	0.40	0.47	0.03
6 o'clock	0.39	0.55	0.57	0.56	0.56	0.49		0.68	0.59	0.55	0.04

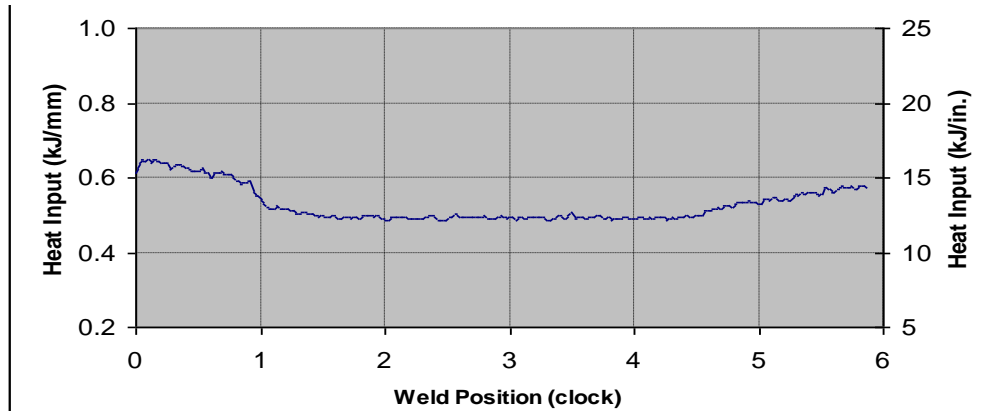
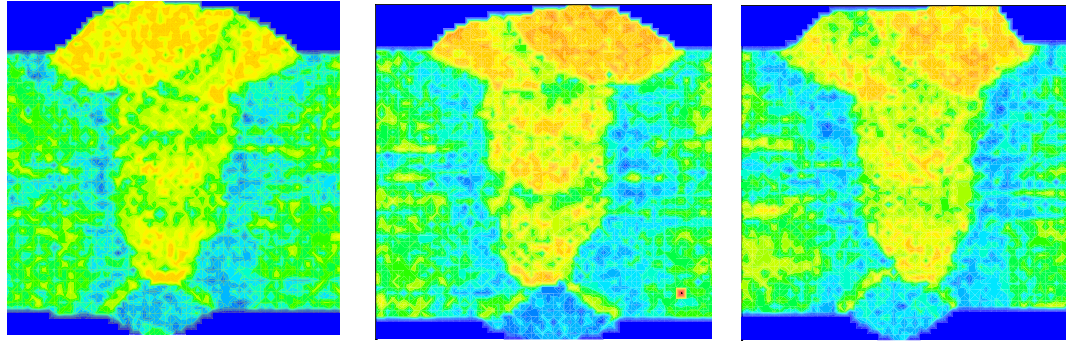


Figure 25. Variation of True Heat Input with clock position, Weld #4 Fill Pass 1

3.5 Tensile & Hardness Results

The tensile properties were measured with a strip tensile specimen, details of which are described by Panday and Daniel [11]. Results obtained from welds made at contractor A are shown in Figure 26(a) & 27(a) and those made at contractor B are shown in Figure 28(a) and 29(a).

Results indicate that the stress strain curves at the 3 and 6 clock positions are very close, while the 12 clock position provides lower values in weld 952-D made by contractor A. This is in spite of the True Heat Input being much lower in the 3 clock position, than the 12:00 or 6:00 clock position as indicated earlier in Table 3. These results, in general, follow the microhardness distributions obtained in the three clock positions, an example of which is shown in Figure 26(b) through 26(d). The microhardness distributions are very similar in the 3 and 6 clock positions with more softening in the 12 clock position. Despite the higher heat input, the penetration at the 6 clock position is lower than at the 3 or 12 clock positions. This is due to the fact that near the 6 clock position, welding is in an overhead position and weld penetration would be lower than in the other clock positions. This causes less re-melting of the prior pass, leaving more as-deposited regions in the weld leading to higher strengths.



b) 12 clock

c) 3 clock

d) 6 clock

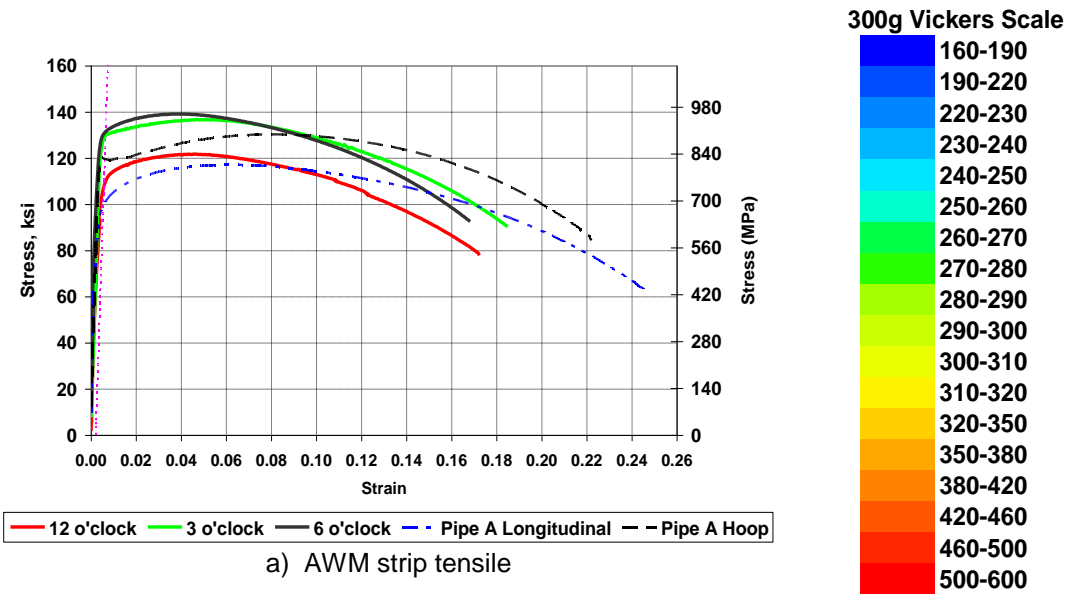


Figure 26. 952-D Stress-Strain Curves and Microhardness Maps (single torch, PT1)

In weld 952-F, the stress strain curves for all three clock positions are right on top of each other as shown in Figure 27(a). This is in spite of the True Heat Input being much lower in the 3 clock position, than the 12 or 6 clock positions as illustrated earlier in Table 4. Once again the higher strengths at the 6 clock position are due to the lower penetration at that position leaving more high strength as-deposited weld metal as shown in Figure 27(d). The microhardness graphs, illustrated in Figures 27(b) through 27(d) further show that while 12 and 6 clock positions show similar hardness distributions, significant softening is observed in the 3 clock position, and this is not reflected in its stress strain behavior, which seems a little puzzling. The observed correlation differences could be due to a couple of reasons. There is significant variation in the true heat input within a pass and from pass to pass in the 12 and 3 clock positions as shown earlier in Tables 3 and 4. Additionally, the hardness distribution is measured not on the strip tensile specimen, but on a macro slice next to it. Because it cannot be measured on the strip tensile specimen before tensile testing, in 5G welds, the microhardness distribution from the macros slice has to be used as a general trending tool rather than a precise predictor of tensile properties.

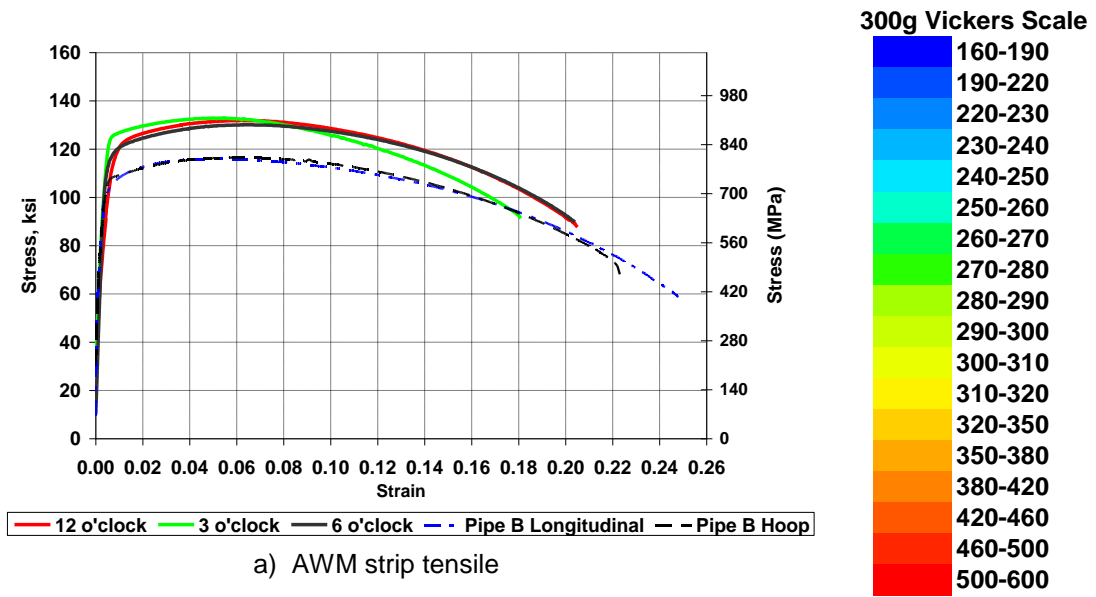
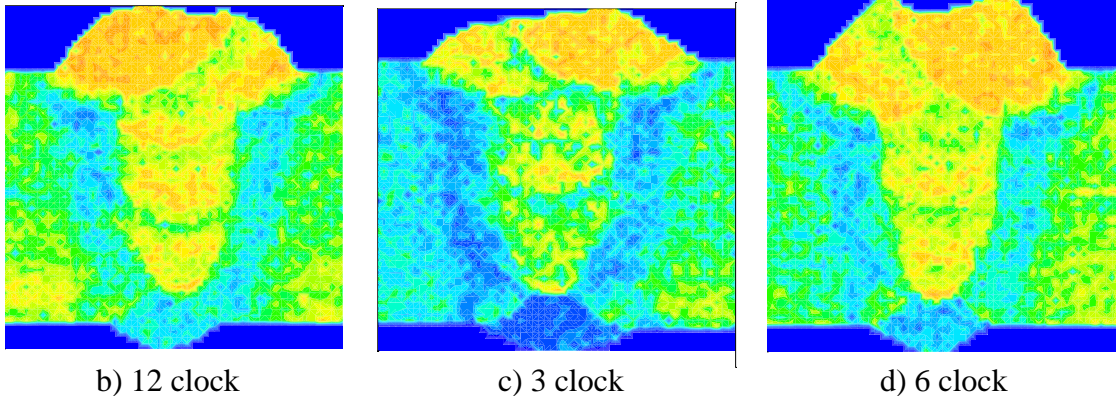


Figure 27. 952-F Stress-Strain Curves and Microhardness Maps (single torch, PT1)

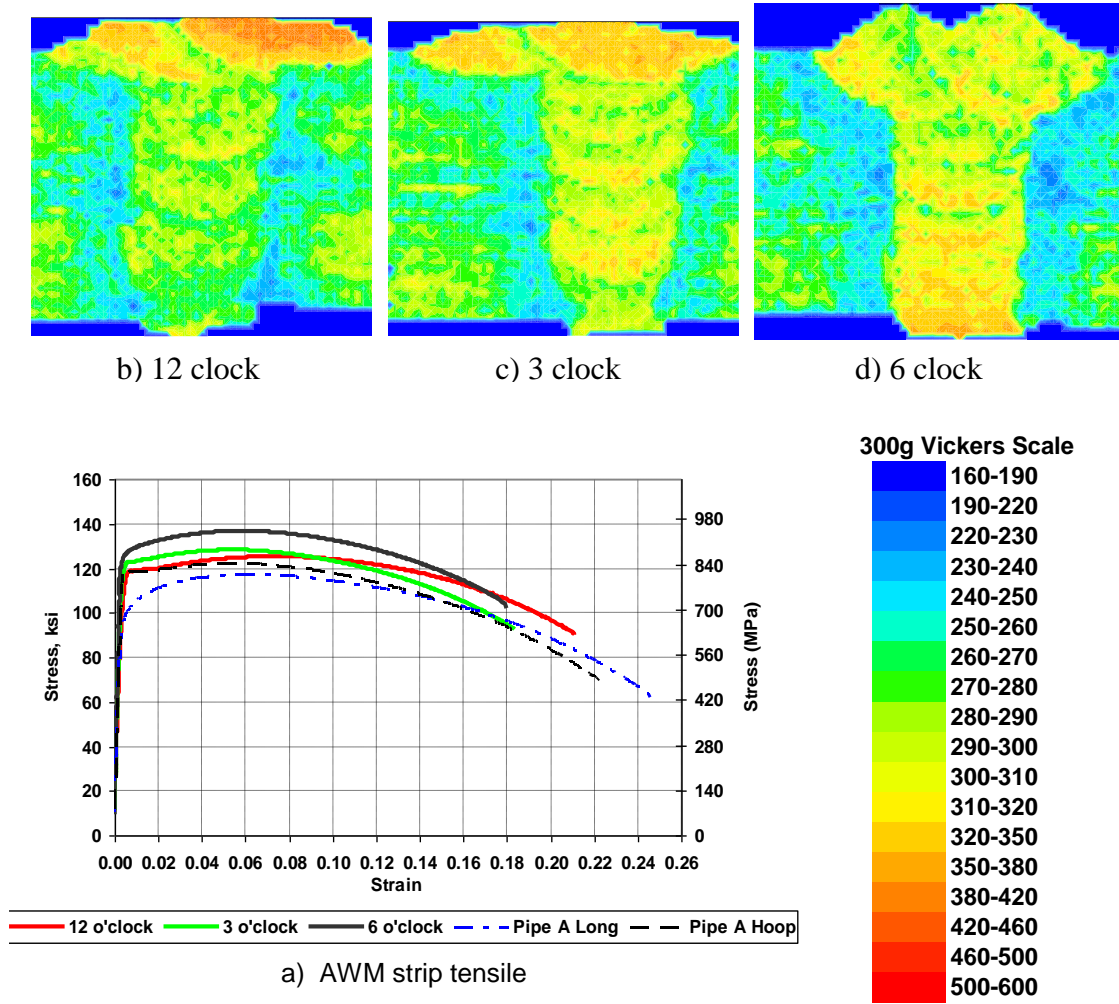


Figure 28. Weld 3 Stress-Strain Curves and Microhardness Maps (single torch, PT1)

Welds made by contractor B produced tensile properties that are similar at 12 and 3 o'clock positions, but produce higher tensile results at 6 o'clock as shown in Figures 28(a) and 29(a). This is because in addition to the lower penetration with the 6 o'clock position, in the case of the welds made by contractor B, the cap passes in the 6 o'clock position were not fully aligned with the top of the groove, resulting in a significant amount of as-deposited region of higher hardness that did not undergo any softening in the upper portion of the joint, as shown in the microhardness graphs in Figure 28(d) and 29(d).

The strengths in the other clock positions follow the trends observed in the microhardness distributions shown in Figures 28(b) through 28(d) and 29(b) through 29D. In general, except for clock position 6, the tensile properties in the other positions are slightly lower than obtained with contractor A. This is because the weld metal compositions were slightly leaner in Mn and Ti than welds made by Contractor A, because of alloy loss due to the higher %CO₂ in the shielding gas, as seen in Table 7.

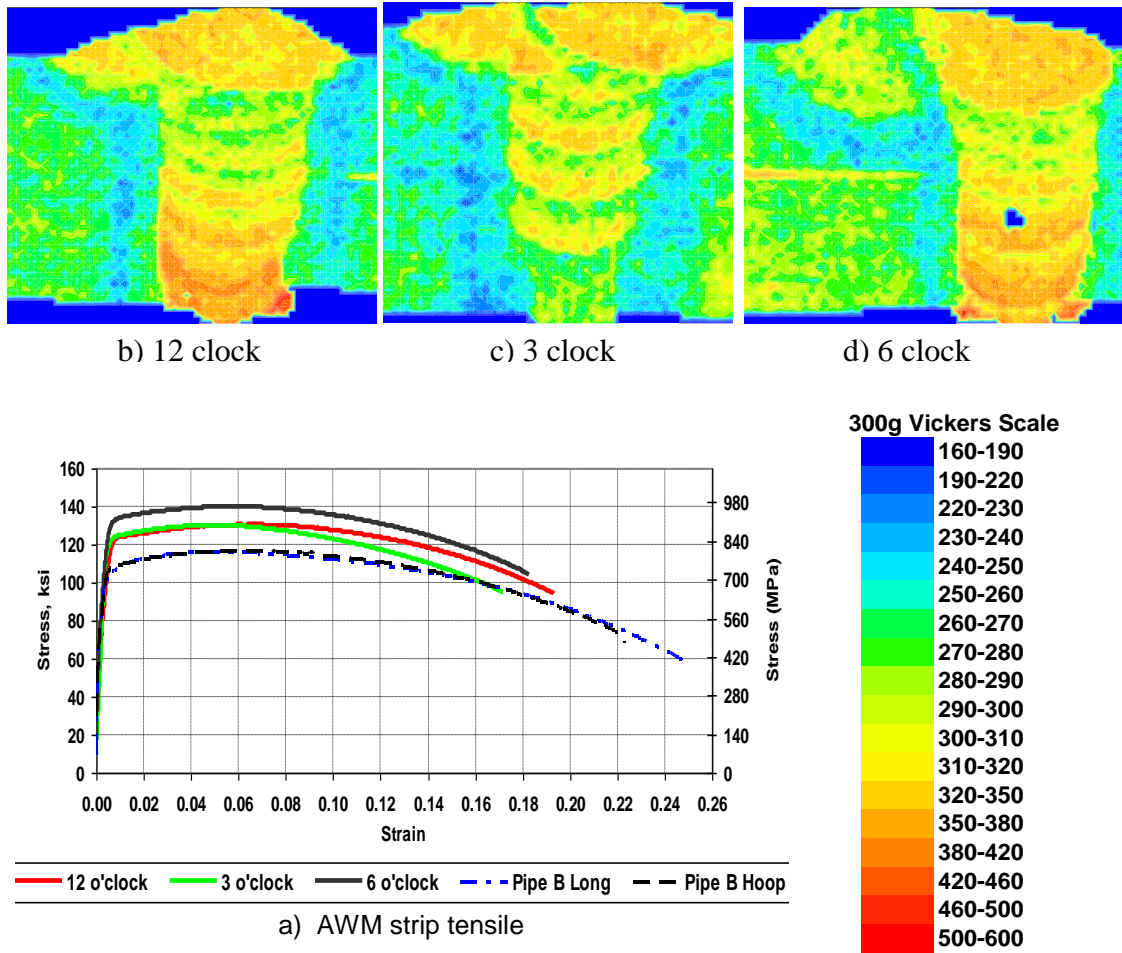


Figure 29. Weld 4 Stress-Strain Curves and Microhardness Maps (single torch, PT1)

With welds at both contractors, in all cases, the weld metal stress strain curves overmatch the longitudinal pipe stress strain curves and in most cases the hoop stress strain curves. This indicates the weld composition provided by PT1 is in a regime where its strength remains high regardless of the differences in pass sequence and cooling behavior at the different clock positions around the pipe in these 5G narrow gap welds.

These results are summarized in Figures 30 and 31 where the 0.2% yield strength, flow stress at 1% total strain (1% flow stress) and tensile strengths are plotted against the true heat inputs with clock positions delineated in them. There is some scatter associated with the reported 0.2% offset yield strength in welds made by both contractors. This could be an artifact of the process of testing the strip tensile specimens for the following reasons. The thinner gage cross section area 4.8 mm x 7.9 mm (0.19 in. x 0.31 in.) combined with asymmetrical geometry of the strip tensile specimen compared to a round specimen can render the test vulnerable to some variation in its early part in the linear elastic range. Since the 0.2% yield strength calculation is based on the slope of the linear elastic portion of the stress strain curve, any testing related variation in this elastic portion can cause this slope to differ significantly from the elastic modulus. This can result in variations in the reported yield strength from similar stress strain curves. However, it is

interesting to see that the flow stress measured at 1% total strain from the stress strain curve is very consistent and mirrors the variation in tensile strength quite well. At 1% total strain, the stress strain curve is out of the linear range, and in the steady state plastic portion. The resulting flow stress is not vulnerable to testing related variation in the elastic range. As a result, for strip tensile specimens ≤ 5.1 mm (≤ 0.2 in.) thick and possibly also circular tensile specimens of ≤ 5.1 mm (≤ 0.2 in.) in diameter) small cross sections, the 1% flow stress may be a more consistent indicator of yield behavior in X100 welds until the testing methodology is refined enough to eliminate the variations in the elastic range.

In the range of heat inputs utilized in these welds, no general trends are evident between the strengths and the heat inputs because of the influence of clock position. The highest strengths obtained with welds made by contractor A are in the 3 and 6 clock positions. The higher strengths at 3 clock positions are by virtue of the lower heat input, and the higher strengths at the 6 clock position are by virtue of the decreased penetration even at the higher heat input. The highest strengths obtained with welds made by contractor B are also in the 3 and 6 clock positions with the 6 clock position providing the highest strength for the reasons mentioned before. There seems to be more scatter in the results in welds from contractor A compared to that from contractor B due to the increased variation in True Heat Input with clock position with the former. These results indicate that in addition to the variables already identified, in 5G welds, there is an additional variable of clock position which can affect the mechanical properties of the weld. However, better control of heat input would provide less scatter in mechanical properties at the different clock positions around the weld.

Analysis of the HAZ softening reveals that there is significant softening as illustrated in Figures 26(b) through 26(d) for weld 952-D (with pipe A), Figures 27(b) through 27(d) for weld 952-F (with pipe B) made by contractor A, Figures 28(b) through 28(d) for weld 3 (with pipe A) and Figures 29(b) through 29(d) for weld 4 (with pipe B) made by contractor B. In weld 952-D, for example, HAZ hardness goes down to values as low as 200-210 VHN in some areas, while most of the HAZ exhibits hardness values in the 220-260 VHN range. In comparison, the weld metal hardness is in the 320-370 VHN range in the as-deposited region, and 250-290 VHN in the reheated region. The hardness distribution in weld 952-F (made with pipe B) was similar. An example of a transverse hardness traverse at the 12 clock position that highlights these observations is shown in Figure 32. Similar HAZ hardness distribution was observed in welds made with Pipe A and B by contractor B and results are shown in Figure 33. No significant differences were detected in the extent of HAZ softening between Pipe A and Pipe B between either contractor A or contractor B. This implies that for single torch welding, the differences in pass sequencing, heat input, preheat and interpass temperatures were not significant enough to make a difference in the extent of HAZ softening in the aforementioned welds with Pipe A and Pipe B.

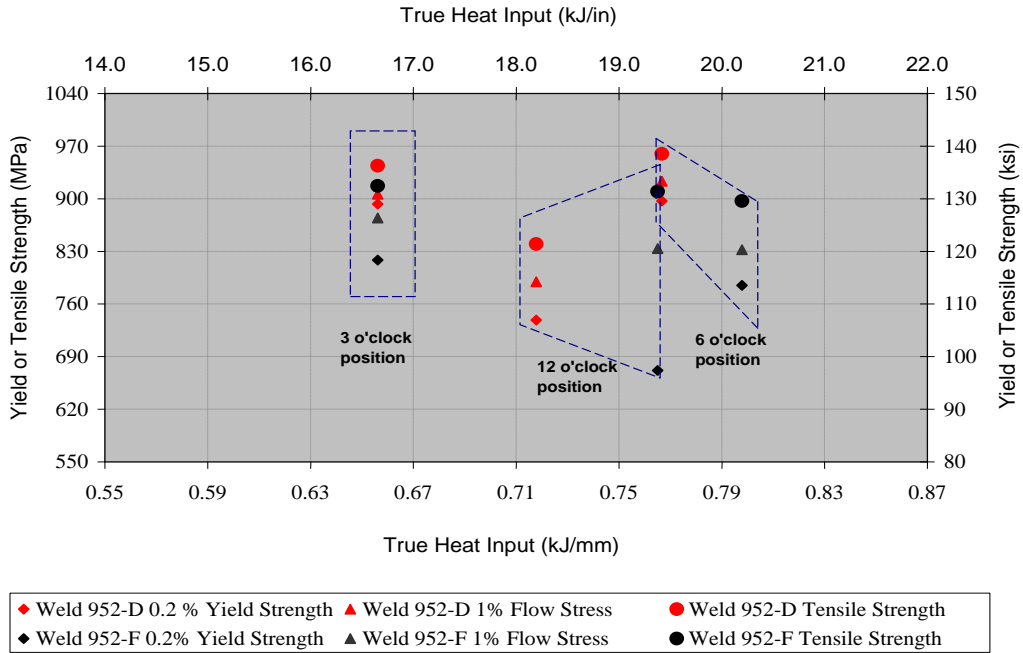


Figure 30. 0.2% Offset Yield Strength, 1% Flow Stress and Tensile Strengths vs. True Heat Input – Contractor A

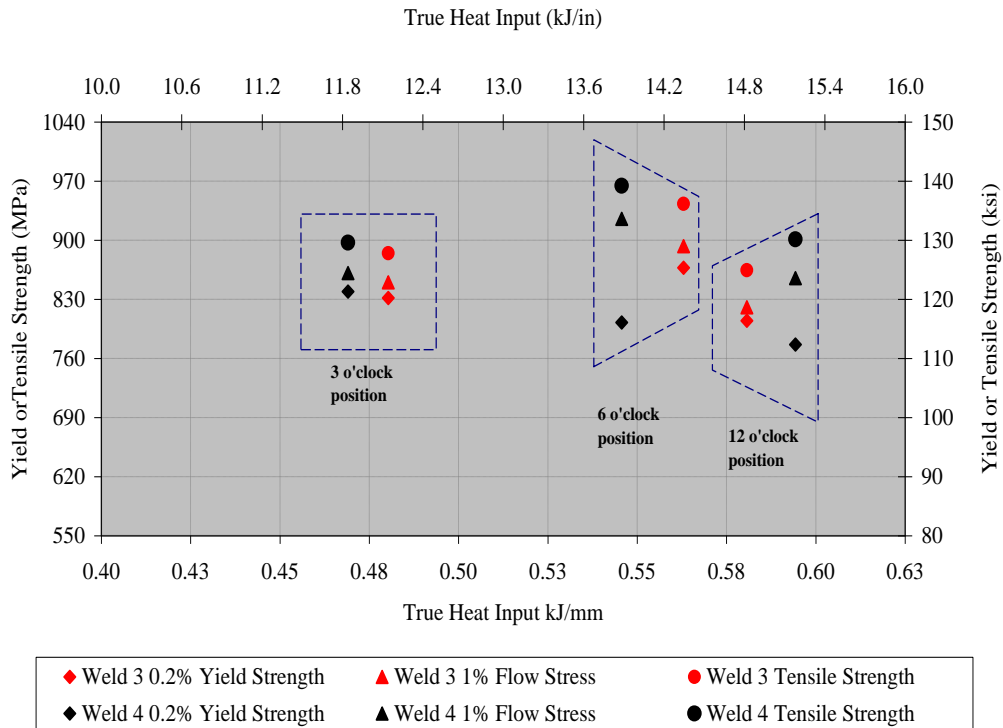


Figure 31. 0.2% Offset Yield Strength, 1% Flow Stress and Tensile Strengths vs. True Heat Input – Contractor B

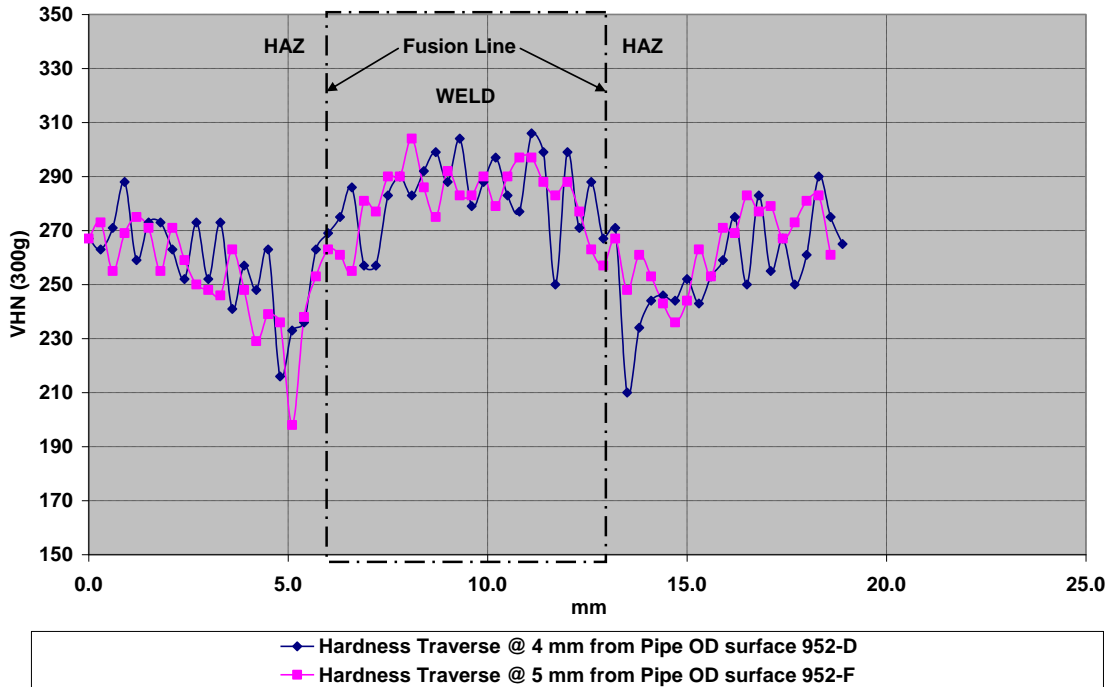


Figure 32. Transverse Microhardness of Single Torch Welds 952-D & 952-F @ 12 o'clock - Contractor A

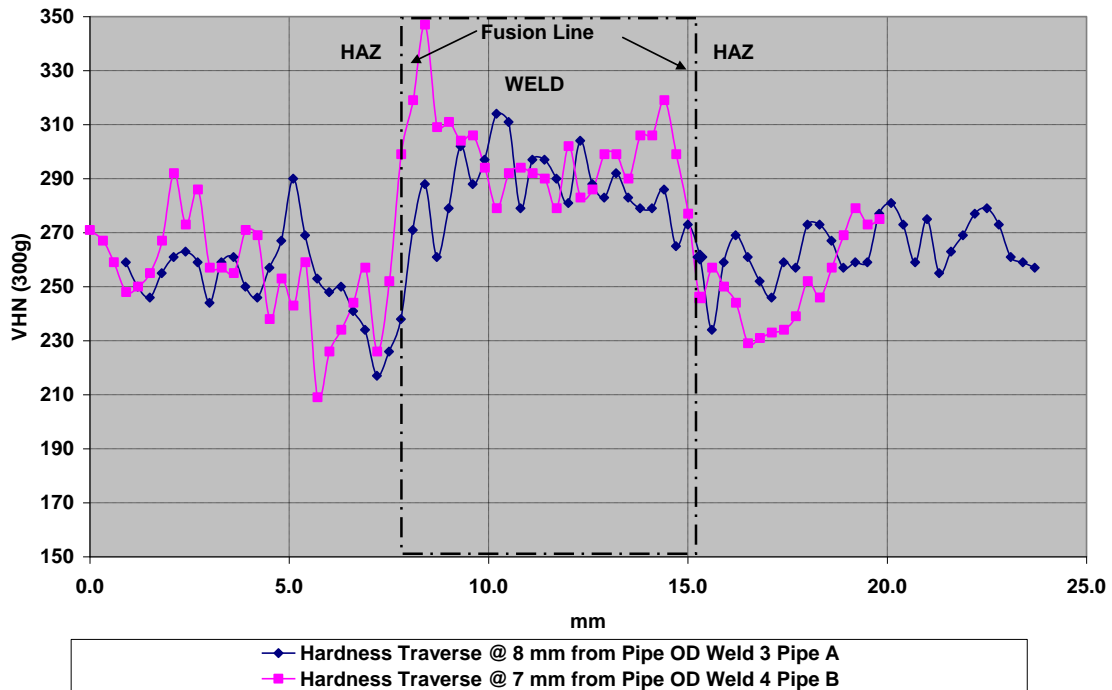


Figure 33. Transverse Microhardness Traverse of Single Torch Welds 3 & Weld 4 @ 12 o'clock - Contractor B

3.6 Impact Toughness

Charpy toughness at -20°C (represented as an average of three results) for weld metal made by contractor A was in the range of 145-245 J for pipe A and 165-225 J for pipe B. It seems that as the True Heat Input is increased, the weld metal Charpy toughness increases as seen in the dashed trend lines in Figure 34. Interestingly, the highest heat input also happens to be at the 6 clock position which provides high strength in the weld metal; therefore the increase in weld metal Charpy toughness is not due to a general softening, but presumably due to a higher toughness as-deposited microstructure with the PT1 consumable. The corresponding HAZ Charpy toughness values were in the range of 130-285 J for pipe A and 255-270 J for pipe B. These results are illustrated in Figure 34.

Welds made by contractor B provided corresponding toughness values in the range of 90-120 J for pipe A and 95-185 J for pipe B as shown in Figure 35. The corresponding HAZ Charpy toughness values were in the range of 180-250 J for Pipe A and 240-270 J for pipe B. No general trend of weld metal Charpy toughness is seen with True Heat Input. In general, the weld metal Charpy toughness at the 6 clock position seems higher than at 12 and 3 clock positions. This higher toughness also comes with the highest strengths at the 6 clock positions, and, as mentioned before, the increase in toughness is not due to softening, but presumably due to a higher toughness as-deposited microstructure with the PT1 consumable.

In general, weld metal and HAZ Charpy toughness values obtained in both welds are quite high, barring some occasional low values in the HAZ. The lower weld metal Charpy toughness values from welds made by contractor B are due to the higher % CO_2 in the shielding gas mixture resulting in higher oxygen levels in the weld metal. There was no significant difference in HAZ Charpy toughness as True Heat Input varied in welds made by either contractor. The difference in HAZ toughness between Pipe A and Pipe B does not seem to be significant.

It seems that in these welds the clock position has an effect on the Charpy toughness, whereby the 6 clock position provides higher toughness, followed by the 3 clock position and then the 12 clock position. Increasing the True Heat Input does seem to help increase the weld metal Charpy toughness, but there is an interaction effect with clock position which complicates the analysis. Details of all chemical compositions and mechanical property results are listed in Tables 7 and 8 respectively.

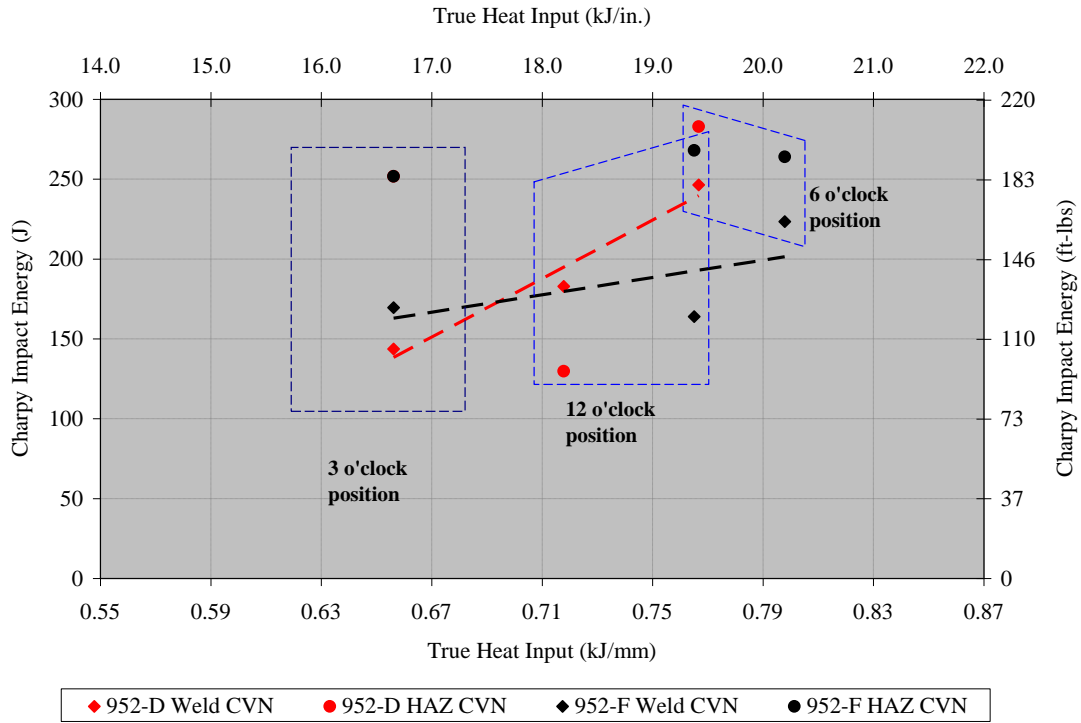


Figure 34. Charpy v-notch impact strength as a function of True Heat Input and Clock Position – Contractor A

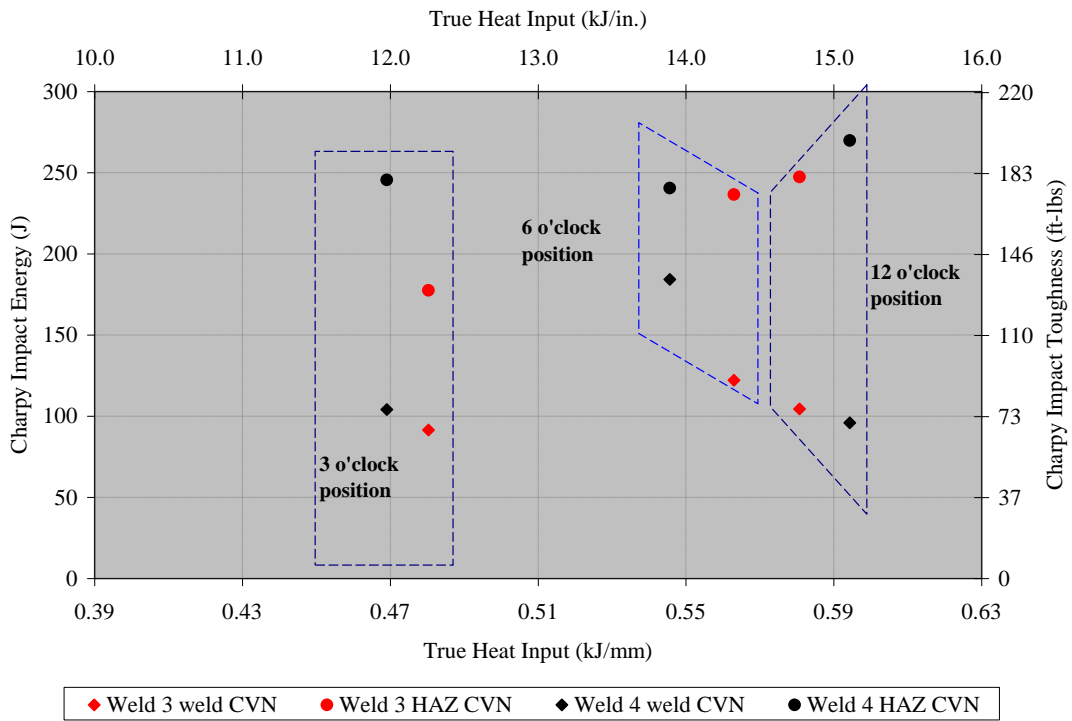


Figure 35. Charpy v-notch impact strength as a function of True Heat Input and Clock Position – Contractor B

4 CONCLUSIONS

The essential welding variables for X100 welding have been identified using the thermal-microstructure model. The model provides robust predictions for thermal behavior, however, it needs refinement as far as the microstructure and hardness predictions are concerned. Further refinement will increase its effectiveness as a screening tool to identify the primary welding variables that effect weld hardness in high strength pipe welding.

Plate welding experiments using statistical design of experiments have corroborated the predictions of the model, providing further insight into the correlations between the primary variables and mechanical properties of the weld. The primary variables are weld metal composition, preheat and interpass temperature, True Heat Input, and torch configuration. True Heat Input, rather than the conventional average heat input, has been demonstrated to be a more accurate measure of the heat input into the weld, especially with pulse welding waveforms. Groove offset has not been identified as a significant variable. The correlations between the primary welding variables and weld mechanical properties can be described very well with linear models. The associated transfer functions have enabled the determination of control limits for the welding variables, for a given weld metal composition, to obtain the weld mechanical properties such as yield and tensile strengths within desired ranges. This has enabled the development of a control methodology for the essential welding variables.

Implementation of the control methodology for the essential welding variables in field welding practice is not easy, but is feasible, provided the True Heat Input during welding is monitored and controlled within the prescribed limits with appropriate instrumentation, and the preheat and interpass temperature is controlled within the prescribed limits. However, in 5G welding, there seems to be an effect of clock position on both the strength and the toughness of the welds, which goes beyond what can be explained by True Heat Input variation alone. This effect of clock position can provide more variation in the mechanical properties of the weld. However, following the control methodology to reduce the variation in True Heat Input as a function of clock position will help in reducing the overall variation in mechanical properties.

Table 7. Chemical Composition of Single Torch Welds made during Shop Welding to mimic Field Welding

Weld ID	Clock Position	%C	%Mn	%Si	%Ti	%Cr	%Mo	%Ni	%N	%O	%S	%P	%Cu	%Nb	CE IIW	Pcm	Cen	Bs	Ms
Welds made by Contractor A																			
952-D	12	0.085	1.63	0.49	0.037	0.17	0.42	1.3	0.004	0.039	0.009	0.015	0.18	0.008	0.574	0.252	0.379	565	433
952-D	3	0.084	1.63	0.49	0.034	0.17	0.42	1.24	0.004	0.037	0.008	0.015	0.18	0.01	0.569	0.250	0.375	568	435
952-D	6	0.09	1.67	0.50	0.038	0.16	0.4	1.14	0.004	0.030	0.008	0.015	0.19	0.012	0.569	0.254	0.388	569	433
Welds made by Contractor B																			
952 F	12	0.086	1.66	0.47	0.032	0.29	0.38	1.27	0.004	0.032	0.008	0.014	0.25	0.006	0.598	0.259	0.395	559	431
952 F	3	0.084	1.63	0.44	0.032	0.29	0.37	1.24	0.007	0.028	0.008	0.014	0.25	0.006	0.588	0.254	0.384	564	434
952 F	6	0.087	1.67	0.48	0.035	0.28	0.37	1.22	0.004	0.03	0.007	0.013	0.25	0.006	0.594	0.260	0.395	561	431
Welds made by Contractor B																			
Weld 3	12	0.085	1.52	0.46	0.029	0.18	0.43	1.29	0.005	0.052	0.007	0.015	0.21	0.009	0.561	0.248	0.371	574	437
Weld 3	3	0.083	1.48	0.45	0.027	0.19	0.44	1.36	0.005	0.051	0.006	0.015	0.19	0.007	0.559	0.245	0.365	574	437
Weld 3	6	0.094	1.50	0.47	0.030	0.19	0.44	1.37	0.005	0.039	0.006	0.016	0.28	0.007	0.581	0.262	0.401	569	431
Welds made by Contractor B																			
Weld 4	12	0.089	1.48	0.46	0.027	0.24	0.44	1.44	0.005	0.063	0.008	0.014	0.41	0.004	0.596	0.266	0.398	566	432
Weld 4	3	0.092	1.56	0.43	0.027	0.28	0.39	1.31	0.004	0.040	0.006	0.013	0.24	0.006	0.590	0.260	0.402	564	431
Weld 4	6	0.093	1.52	0.46	0.029	0.25	0.42	1.41	0.004	0.049	0.006	0.014	0.52	0.004	0.609	0.276	0.416	564	430

Table 8. Mechanical Properties of Single Torch Welds made during Shop Welding to mimic Field Welding

Weld ID	Clock Position	Mean True Heat Input HI _{TE} for All Fill Passes kJ/in	Std Dev of HI _{TE} for All Fill Passes kJ/in	Mean True Heat Input HI _{TE} for All Fill Passes kJ/mm	Std Dev of HI _{TE} for All Fill Passes kJ/mm	0.2% Yield, ksi	0.2% Yield, MPa	Flow Stress @ 1% Total Strain, ksi	Flow Stress @ 1% Total Strain, MPa	UTS, ksi	UTS, MPa	Weld Metal CVN @ -20°C (J)			Average (J)	Average (ft-lbs)	HAZ CVN @ -20°C (J)			Average (J)	Average (ft-lbs)
Welds made by Contractor A																					
952-D	12	18.2	2.0	0.72	0.08	107	738	115	789	122	840	202	178	171	183	135	240	89	61	130	96
952-D	3	16.7	2.0	0.66	0.08	130	893	131	906	137	944	145	142	145	144	106	248	245	264	253	186
952-D	6	19.5	1.0	0.77	0.04	130	897	134	923	139	960	229	296	217	247	182	281	278	293	284	209
Welds made by Contractor B																					
952 F	12	19.4	0.2	0.77	0.01	97	672	121	834	132	909	159	172	163	165	121	254	282	271	269	198
952 F	3	16.7	2.3	0.66	0.09	119	818	127	874	133	917	171	169	-	170	126	218	279	260	253	186
952 F	6	20.3	0.8	0.80	0.03	114	785	121	832	130	897	199	240	233	224	165	264	251	279	265	195
Welds made by Contractor B																					
Weld 3	12	14.8	0.6	0.58	0.03	117	805	119	820	125	865	102	108	104	105	77	243	249	252	248	183
Weld 3	3	12.2	0.8	0.48	0.03	121	832	123	850	128	885	95	95	85	92	68	168	194	172	178	131
Weld 3	6	14.3	0.3	0.56	0.01	126	867	130	893	137	943	127	123	117	122	90	233	239	240	237	175
Welds made by Contractor B																					
Weld 4	12	15.1	0.3	0.59	0.01	113	776	124	855	131	901	91	100	98	96	71	267	271	274	271	200
Weld 4	3	11.9	0.7	0.47	0.03	122	839	125	861	130	897	113	107	94	104	77	236	228	275	246	182
Weld 4	6	13.9	0.8	0.55	0.03	116	803	134	925	140	965	226	171	157	185	136	249	224	251	241	178

5 REFERENCES

- 1) Hammond, J., “State of The Art Review”, Final Report 278-T-01 to PHMSA per Agreement # DTPH56-07-000005, September 2011.
- 2) Hudson, M.G., Blackman, S.A., Hammond, J., Dorling, D.V., “Girth welding of X100 pipeline steels”, Paper IPC2002-27296, Proc. of IPC’02, 4th International Pipeline Conference, Calgary, Alberta, pp. 1-8, 2002.
- 3) Hammond, J., Blackman, S.A., Hudson, M.G., “Challenges of girth welding X100 linepipe for gas pipelines” Proceedings of Pipe Dreamer’s Conference, Yokohama, Japan, pp. 1-25, 2002.
- 4) Hudson, M.G., Blackman, S.A., Hammond, J., Dorling, D.V., “Selection of welding consumables for higher strength steel pipelines”, 4th international Conference on Pipeline Technology, Ostend, Belgium, pp. 1187-1205, 2004.
- 5) Blackman, S.A., Liratzis, T., Howard, R.D., Hudson, M.G., Dorling, D.V., “Recent tandem welding developments for pipeline girth welds”, 4th international Conference on Pipeline Technology, Ostend, Belgium, pp. 335-355, 2004.
- 6) Hudson, M.G., “Welding of X100 line pipe”, Ph.D. Thesis, Welding Engineering Research Centre, Cranfield University, 2004.
- 7) Gianetto, J.A., Bowker, J.T., Dorling, D.V., and Horsley, D., “Structure and properties of X80 and X100 pipeline girth welds. “Paper IPC04-0316, Proc. of IPC 2004, International Pipeline Conference, Calgary, Alberta, 2004.
- 8) Gianetto, J.A., Bowker, J.T., Dorling, D.V., Taylor, D., Horsley, D., Fiore, S.R., “Overview of tensile and toughness testing protocols for assessment of X100 pipeline girth welds” Paper IPC2008-64668, Proc. of IPC 2008, 7th International Pipeline Conference, Calgary, Alberta, Canada 2008.
- 9) Gianetto, J.A., Goodall, G.R., Tyson, W.R., Quintana, M.A., Rajan, V.B. and Chen, Y., “Microstructure and Properties of Simulated Weld Metals”, Final Report 278-T-04 to PHMSA per Agreement # DTPH56-07-000005, September 2011.
- 10) Gianetto, J.A., Goodall, G.R., Tyson, W.R., Quintana, M.A., Rajan, V.B. and Chen, Y., “Microstructure and Properties of Simulated Heat Affected Zones”, Final Report 278-T-05 to PHMSA per Agreement # DTPH56-07-000005, September 2011.
- 11) Panday, R. and Daniel, J., “Materials Selection, Welding and Weld Monitoring”, Final Report 278-T-02 to PHMSA per Agreement # DTPH56-07-000005, September 2011.
- 12) Rajan, V.B., Daniel, J., Chen, Y., Quintana, M., Souza, A., “Welding process selection and control for high strength pipeline applications”, Paper IBP 1506_09, Rio Pipeline Conference and Exhibition 2009, Rio de Janeiro, Brazil, September 2009.
- 13) Chen, Y., Wang, Y.-Y., Quintana, M.A., Rajan, V.B. and Gianetto, J.A., “Thermal Model for Welding Simulations”, Final Report 278-T-07 to PHMSA per Agreement # DTPH56-07-000005, September 2011.
- 14) Chen, Y., Wang, Y.-Y., Quintana, M.A., Rajan, V.B. and Gianetto, J.A., “Microstructure Model for Welding Simulations, Final Report 278-T-08 to PHMSA per Agreement # DTPH56-07-000005, September 2011.
- 15) Chen, Y., Wang, Y.-Y., Rajan, V.B., Quintana, M.A., “Thermal simulation and its experimental verifications for girth welds in high-strength pipelines”, Paper IPC 2010-31373, Proceedings of the 8th International Pipeline Conference, , Calgary, Alberta, Canada, 2010.

- 16) Chen, Y., Wang, Y.-Y., Gianetto, J.A., Rajan V.B., Quintana, M.A., “Simulations for microstructure evolution and its experimental verifications for girth welds in high strength pipelines”, Paper IPC 2010-31374, Proceedings of the 8th International Pipeline Conference, Calgary, Alberta, Canada, 2010.
- 17) Rajan, V.B., Daniel, J., “Application to Other Welding Processes”, Final Report 278-T-09 to PHMSA per Agreement DTPH56-07-000005, September 2011.

6 APPENDIX 1

Virtual Experiment Simulation Matrix

Run No.	Bevel Offset/Bevel Angle	Preheat/Interpass Temp	Torch Configuration	Weld Procedure	Total No. of Passes excluding Root	WFS/TS Ratio per pass - All fill passes	Estimated Average Heat Input per fill pass kJ/in	Estimated Average Heat Input per fill pass kJ/mm	Estimated True heat Input per fill pass kJ/in	Estimated True heat Input per fill pass kJ/mm	Estimated True Heat Input/(WFS/TS) Ratio for each fill pass	Consumable Composition Pcm
1	.090/5 deg bevel	100C/100C	Single	A	11	13	8	0.31	9	0.35	0.72	0.25
2	.090/5 deg bevel	100C/100C	Single	B	7	24	15	0.59	18	0.71	0.73	0.25
3	.090/5 deg bevel	180C/180C	Single	A	11	13	8	0.31	9	0.35	0.72	0.25
4	.090/5 deg bevel	180C/180C	Single	B	7	24	15	0.59	18	0.71	0.73	0.25
5	.090/5 deg bevel	27C/27C	Single	A	11	13	8	0.31	9	0.35	0.72	0.25
6	.090/5 deg bevel	27C/27C	Single	B	7	24	15	0.59	18	0.71	0.73	0.25
7	.110/5 deg bevel	100C/100C	Single	C	12	13	8	0.31	9	0.35	0.72	0.25
8	.110/5 deg bevel	100C/100C	Single	D	7	24	15	0.59	18	0.71	0.73	0.25
9	.110/5 deg bevel	180C/180C	Single	C	12	3	8	0.31	9	0.35	0.72	0.25
10	.110/5 deg bevel	180C/180C	Single	D	7	24	15	0.59	18	0.71	0.73	0.25
11	.110/5 deg bevel	27C/27C	Single	C	12	13	8	0.31	9	0.35	0.72	0.25
12	.110/5 deg bevel	27C/27C	Single	D	7	24	15	0.59	18	0.71	0.73	0.25
13	.090/5 deg bevel	100C/100C	Dual	E	11	13	8	0.31	9	0.35	0.72	0.25
14	.090/5 deg bevel	100C/100C	Dual	F	7	24	15	0.59	18	0.71	0.73	0.25
15	.090/5 deg bevel	180C/180C	Dual	E	11	13	8	0.31	9	0.35	0.72	0.25
16	.090/5 deg bevel	180C/180C	Dual	F	7	24	15	0.59	18	0.71	0.73	0.25
17	.090/5 deg bevel	27C/27C	Dual	E	11	13	8	0.31	9	0.35	0.72	0.25
18	.090/5 deg bevel	27C/27C	Dual	F	7	24	15	0.59	18	0.71	0.73	0.25
19	.110/5 deg bevel	100C/100C	Dual	G	12	13	8	0.31	9	0.35	0.72	0.25
20	.110/5 deg bevel	100C/100C	Dual	H	7	24	15	0.59	18	0.71	0.73	0.25
21	.110/5 deg bevel	180C/180C	Dual	G	12	13	8	0.31	9	0.35	0.72	0.25
22	.110/5 deg bevel	180C/180C	Dual	H	7	24	15	0.59	18	0.71	0.73	0.25
23	.110/5 deg bevel	27C/27C	Dual	G	12	13	8	0.31	9	0.35	0.72	0.25
24	.110/5 deg bevel	27C/27C	Dual	H	7	24	15	0.59	18	0.71	0.73	0.25
25	.090/5 deg bevel	27C/27C	Single	A	11	13	8	0.31	9	0.35	0.72	0.25
26	.090/5 deg bevel	180C/180	Single	B	7	24	15	0.59	18	0.71	0.73	0.25
27	.110/5 deg bevel	27C/27C	Single	C	12	13	8	0.31	9	0.35	0.72	0.25
28	.110/5 deg bevel	180C/180	Single	D	7	24	15	0.59	18	0.71	0.73	0.25
29	.090/5 deg bevel	27C/27C	Dual	E	11	13	8	0.31	9	0.35	0.72	0.25
30	.090/5 deg bevel	180C/180	Dual	F	7	24	15	0.59	18	0.71	0.73	0.25
31	.110/5 deg bevel	27C/27C	Dual	G	12	13	8	0.31	9	0.35	0.72	0.25
32	.110/5 deg bevel	180C/180	Dual	H	7	24	15	0.59	18	0.71	0.73	0.25
33	.090/5 deg bevel	27C/27C	Single	A	11	13	8	0.31	9	0.35	0.72	0.25
34	.090/5 deg bevel	180C/180	Single	B	7	24	15	0.59	18	0.71	0.73	0.25
35	.110/5 deg bevel	27C/27C	Single	C	12	13	8	0.31	9	0.35	0.72	0.25
36	.110/5 deg bevel	180C/180	Single	D	7	24	15	0.59	18	0.71	0.73	0.25
37	.090/5 deg bevel	27C/27C	Dual	E	11	13	8	0.31	9	0.35	0.72	0.25
38	.090/5 deg bevel	180C/180	Dual	F	7	24	15	0.59	18	0.71	0.73	0.25
39	.110/5 deg bevel	27C/27C	Dual	G	12	13	8	0.31	9	0.35	0.72	0.25

Virtual Experiment Simulation - Analysis of Variance

Source	Sum of Squares	df	Mean Square	F Value	p-value Prob >F	
Model	3307.38	5	661.48	24.99	< 0.0001	significant
A-Preheat/interpass	1684.75	1	1684.75	63.66	< 0.0001	
B-Wire Comp	831.1	1	831.1	31.4	< 0.0001	
C-True Energy	1.75	1	1.75	0.066	0.7988	
D-Offset	141.37	1	141.37	5.34	0.027	
E-Torch Configuration	185.26	1	185.26	7	0.0123	
Residual	899.87	34	26.47			
Cor Total	4207.25	39				

Plate Experiments DOE Matrix

Run	Factor 1 Preheat/ Interpass Temp °C	Factor 2 Wire Composition Pcm	Factor 3 Groove Offset, in	Factor 4 True Heat Input kJ/in	Factor 4 True Heat Input kJ/mm	Factor 5 Torch Configuration	True Heat Input/WFS- TS ratio*
1	180	0.22	0.11	11.7	0.46	Single	0.62
2	180	0.22	0.11	14.0	0.55	Single	0.73
3	180	0.22	0.11	21.2	0.83	Single	0.81
4	180	0.22	0.11	23.1	0.91	Single	0.88
5	27	0.33	0.09	13.8	0.54	Single	0.72
6	27	0.22	0.09	12.8	0.50	Single	0.67
7	180	0.22	0.09	21.3	0.84	Single	0.81
8	180	0.33	0.09	12	0.47	Single	0.63
9	27	0.22	0.11	13.8	0.54	Single	0.72
10	104	0.33	0.11	22	0.87	Single	0.84
11	104	0.33	0.11	20.7	0.81	Single	0.79
12	27	0.22	0.09	13.7	0.54	Dual 4" Gap	0.72
13	27	0.28	0.09	22.4	0.88	Dual 4" Gap	0.85
14	27	0.22	0.09	13.7	0.54	Dual 4" Gap	0.72
15	180	0.33	0.09	13	0.51	Dual 7" Gap	0.68
16	27	0.33	0.09	23.2	0.91	Dual 7" Gap	0.88
17	27	0.33	0.11	21.3	0.84	Dual 4" Gap	0.81
18	180	0.33	0.11	23.1	0.91	Dual 4" Gap	0.88
19	180	0.28	0.11	12.8	0.50	Dual 4" Gap	0.67
20	180	0.28	0.11	12.7	0.50	Dual 4" Gap	0.67
21	180	0.22	0.09	22.1	0.87	Dual 4" Gap	0.84
22	104	0.22	0.09	23.4	0.92	Dual 7" Gap	0.89
23	180	0.33	0.09	13.1	0.52	Dual 7" Gap	0.68
24	27	0.22	0.11	21.9	0.86	Dual 7" Gap	0.83
25	180	0.33	0.11	23.2	0.91	Dual 7" Gap	0.88
26	180	0.22	0.11	21.7	0.85	Dual 7" Gap	0.83
27	27	0.33	0.11	12.2	0.48	Dual 7" Gap	0.64
28	180	0.22	0.1	13.7	0.54	Dual 7" Gap	0.72
29	27	0.22	0.1	23.3	0.92	Dual 4" Gap	0.89

*True Heat Input/WFS/TS ratio is provided for information only, to show its variation with the change in True Heat Input brought about by the changes in the WFS/TS ratio and waveform. It was not used in the statistical analysis as an independent input variable; rather True Heat Input itself was used as the input variable for the purpose of clarity.

Chemical Compositions of Pipe Used For Field Welding Conditions

	%C	%Mn	%Si	%Ti	%Cr	%Mo	%Ni	%S	%P	%Al	%Cu	%Nb
Pipe A	0.06	1.90	0.32	0.017	0.04	0.23	0.23	0.003	0.012	0.038	0.240	0.040
Pipe B	0.05	1.97	0.18	0.012	0.56	0.10	0.45	<0.003	0.008	0.016	0.480	0.021

7 APPENDIX 2

Measurement Of Essential Welding Variables

Accurate and complete data collection during the welding operation is essential for proper control of the essential welding variables such that consistent mechanical properties are obtained. Accordingly, all welding operations for this project must be preformed according to the following guidelines

Average Voltage, Average Amperage, and Heat Input

On the surface, the required electrical welding data (voltage, amperage, and heat input) may not seem to be anything out of the ordinary but special considerations need to be followed. They are important because the data needs to accurately reflect the conditions at the arc.

Voltage Measurement (and Welding Voltage Control)

All the welding cables and cable connections have resistances that produce voltages as current flows through them. These voltage drops do not represent the conditions at the arc (the actual arc voltage) and must not be included in the voltage measurement. By locating the voltage measurement points near the arc, the cable/connection voltages will not be included in the measurement:

- Positive voltage measurement point should be at the same location where the welding torch and the electrode cable are connected. This is typically a brass connection block on the wire feeder. The measurement point should NOT be the electrode connection on the welding power source.
- Negative, or ground, voltage measurement point should be directly on the work piece. The measurement point should NOT be the work connection on the welding power source.

It is also preferred to exclude the cable/connection voltages from the welding control. If the welding power source is capable of using remote voltage sense leads, the voltage sense leads should be connected to the same locations as mentioned above. Most pulse welding power sources already have electrode voltage sensing built into the wire feeder. All Power Wave power sources from Lincoln Electric have remote voltage sensing capabilities.

Amperage Measurement

The amperage measurement is more straightforward because the current can be measured on the electrode or work cable without special considerations. However, the measurement device for the amperage must have an adequate frequency range as described in the next section. Most “clamp- on” style ammeters have a frequency range starting at 0 Hz (DC) to 15 Hz and extending up to at least 1 kHz or 2 kHz;

If constant voltage power sources are used, conventional calculations of heat input suffice. However, if pulse waveforms are used an accurate calculation of heat input can only be found by using one of the equations below. The fundamental change with the pulse waveform calculations is to include True Energy, or True Power, that must be found from instantaneous power measurements using one of the following equations:

$$\text{True Heat Input (J/mm)} = \frac{\text{True Energy (J)}}{\text{Length of Weld (mm)}}$$

$$\text{True Heat Input (J/mm)} = \frac{\text{True Power (W or J/s)} * \text{Time (s)}}{\text{Length of Weld (mm)}}$$

Instantaneous power measurements at a rate of **5 kHz to 10 kHz** will create an accurate representation of the conditions occurring in a complex waveform. The product of average voltage and average amperage, as used in the conventional heat input calculation, does not accurately represent the conditions occurring in a complex waveform.

The methods available for measuring True Energy or True Power can be divided into two categories: Commercial Power Meters or Custom Data Acquisition Systems.

Commercial Power Meters

Commercially available power meters that are able to measure True Power with a frequency range starting 0 Hz (DC) to 15 Hz and extending up to at least 1 kHz or 2 kHz can be purchased. For example, the following Fluke meters accurately measure the True Power of a complex welding waveform.

- Fluke 345 Power Quality Clamp Meter
- Fluke 43B Power Quality Analyzer plus a separate current probe. An example of an acceptable current probe is AEMC MR561 AC/DC Current Probe

When selecting a commercially available power meter it is important to look closely at the technical specifications. It must be stated that the power meter can measure True Power (NOT just DC power, kVA, or average power). It must also be stated that the frequency range starts at 0 Hz (DC) to 15 Hz and extends up to at least 1 kHz or 2 kHz. For example, testing was performed on an Extech 382068 Clamp -on Power meter but the results were inaccurate because the frequency range of this meter starts at 45 Hz and only extends up to 500Hz.

Custom Data Acquisition Systems

A custom built data acquisition system can also measure the True Power, along with the average voltage and amperage, but the system must be designed to operate in a welding environment where a large amount of electrical noise is present. A custom built data acquisition system should have a data sampling rate of at least 5 kHz and the calibration accuracy must be verified. The True Power is then calculated by averaging the instantaneous product of each voltage and amperage data sample. A pulse welding power source may have the ability to perform this data acquisition and True Power calculation. All Power Wave power sources from Lincoln Electric have this capability.

Lincoln Electric has a True Energy meter (data acquisition system) that can be used on any power source if a commercial power meter or custom data acquisition system is not available.

Recording the Average Voltage, Average Amperage, and Heat Input

Using a commercial power meter or a custom data acquisition system, the following values must be recorded during all welding operations on this project.

- Average Voltage
- Average Amperage
- True Power

When using a commercial power meter, periodic measurements of these values need to be recorded as the welding operation is performed, for example, every 15 to 30 seconds. Recording these values frequently will demonstrate the consistency of the welding operation and highlight any changes that may occur. A single measurement that is assumed to be the average for the entire weld is not acceptable. When using a custom data acquisition system, the periodic measurements will be performed at a minimum rate of 5 kHz, and the resulting data can be analyzed as needed.